

1 **Unveiling the potential of biomechanics in pioneering innovative strategies for**
2 **cancer therapy**

3 Xiaodong Wu^{1, #}, Weidong Fei^{1, #}, Tao Shen¹, Lei Ye¹, Chaoqun Li¹, Siran Chu², Mingqi Liu¹,
4 Xiaodong Cheng^{1, 3, 4 *}, Jiale Qin^{1, 3, 4 *}

5
6 ¹ Women's Hospital, Zhejiang University School of Medicine, Hangzhou, 310006, China.

7 ² Zhejiang University School of Medicine, Hangzhou, 310000, China.

8 ³ Zhejiang Key Laboratory of Precision Diagnosis and Therapy for Major Gynecological
9 Diseases, Hangzhou, 310006, China.

10 ⁴ Zhejiang Provincial Clinical Research Center for Gynecological Diseases, Hangzhou,
11 310006, China.

12
13 # These authors contributed equally.

14 * E-mail address of corresponding authors: qinjiale@zju.edu.cn (JL. Qin) and
15 chengxd@zju.edu.cn (XD. Cheng).

16
17
18
19
20
21
22
23
24
25
26
27
28
29
30
31

32 **Abstract**

33 Mechanical force transmission is pivotal in tumor biology, profoundly affecting cancer cell
34 behaviors such as proliferation, metastasis, and resistance to therapy. To explore novel
35 biomechanical-based therapeutic strategies for cancer treatment, this paper deciphers the
36 advances in biomechanical measurement approaches and the impact of biomechanical
37 signals on fundamental oncological processes such as tumor microenvironment
38 remodeling, angiogenesis, metastasis, and drug resistance. Then, the mechanisms of
39 biomechanical signal transduction of tumor cells are demonstrated to identify novel targets
40 for tumor therapy. Additionally, this study proposes a novel tumor treatment strategy, the
41 biomechanical regulation tumor nanotherapeutics, including smart biomaterials designed
42 to disturb mechanical signaling pathways and innovative nanodrugs that interfere
43 transduction of biomechanical signals to improve tumor therapeutic outcomes. These
44 methods mark a departure from conventional pharmacological therapies to novel strategies
45 that utilize mechanical forces to impede tumor progression and enhance tumor
46 responsiveness to treatment. In general, this review highlights the critical role of
47 biomechanical signals in cancer biology from a holistic perspective and underscores the
48 potential of biomechanical interventions as a transformative class of therapeutics. By
49 integrating mechanobiology into the development of cancer treatments, this paper paves
50 the way for more precise and effective strategies that leverage the inherent physical
51 properties of the tumor microenvironment.

52

53 **Keywords:** biomechanics, cancer, mechanosensors, mechanosignaling proteins,
54 nanotherapeutics

55

56

57

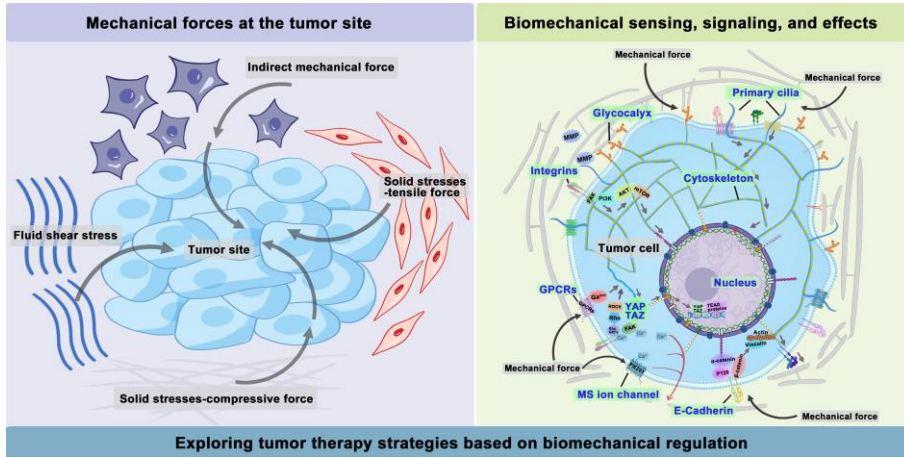
58

59

60

61 **Graphical abstract**

62



Exploring tumor therapy strategies based on biomechanical regulation

63

(Graphics parameters, 12 cm (width) × 6 cm (height), 1000 dpi)

64

65

66

67

68

69

70

71

72 **1. Introduction**

73 Despite significant advancements in anti-cancer drug development, diagnostic
74 methods, and treatment approaches, cancer continues to be the leading cause of mortality
75 worldwide. Cancer has traditionally been understood as primarily stemming from genetic
76 abnormalities, which trigger epigenetic changes and result in abnormal cellular behaviors
77 [1]. However, the role of cellular physical properties in cancer initiation and progression
78 has recently attracted scientific attention. Biomechanics, especially the mechanical
79 microenvironment of tumors, plays an important role in cancer prediction, diagnosis, and
80 treatment. Tumor cells inhabit abnormal mechanical microenvironments, including altered
81 solid tumor stress, extracellular matrix (ECM) stiffness, and hydrostatic pressure [2]. Tumor
82 cells sense and convert these mechanical signals into biochemical signals through
83 mechanosensors, which include glycocalyx, primary cilia, cytoskeleton, and nucleus. Any
84 disturbance to this mechanotransduction may result in tumor progression. Many
85 biophysicists can predict cellular activities such as division, proliferation, metastasis, and
86 drug resistance through the physical characteristics of tumor cells accurately [3, 4].
87 Therefore, integrating theoretical and experimental approaches from mechanics and
88 biology into tumor biomechanics allows for a detailed investigation of the complex
89 mechanical dynamics underlying cancer [5].

90 To achieve the transition from specific mechanosensitive (MS) molecules to tumor
91 mechanomedicine, this article elucidates how the tumor mechanical environment impacts
92 their growth and progression, from molecular and subcellular to cellular, tissue, organ, and
93 even whole-body scales perspective. Firstly, this paper elucidates the biomechanical
94 measurement approaches, biomechanical characteristics of tumor tissue, and how
95 biomechanics promote tumor progression. Then, the manuscript decodes the
96 biomechanical signaling mechanisms of cancer cells. The cellular mechanosensors in
97 tumor cells, like glycocalyx and primary cilia, are responsible for sensing mechanical
98 signals in the tumor microenvironment. After that, diverse mechanosignaling proteins are
99 responsible for transmitting biomechanical signals inside tumor cells to achieve better
100 survival. During the above process, this article summarizes a series of potential or clinically
101 studied anti-tumor small molecule drugs that interfere with mechanical signal reception or
102 conduction (**Table 1**). Based on the published research, this paper summarizes a novel

103 tumor treatment strategy: the biomechanical regulation tumor nanotherapeutics, which
104 aims to achieve tumor treatment by blocking the biomechanical signal transduction through
105 the nanosystems. By adopting a holistic, interdisciplinary, rigorous investigation into the
106 biomechanics of cancer, there exists a substantial opportunity to transform established
107 therapeutic strategies. This could significantly boost cancer treatment efficacy, ultimately
108 elevating survival rates and enriching the life quality of patients.

109 **2. Biomechanical measurement approaches**

110 Accurate measurement of mechanical properties is crucial for studying tumor
111 mechanobiology. Based on the spatial and temporal scales, as well as the force sensitivity
112 characteristics of tumor tissue, various biophysical techniques, such as atomic force
113 microscopy (AFM), micropipette aspiration (MPA), and traction force microscopy (TFM),
114 have been developed to measure stiffness, viscoelasticity, or deformability, shedding light
115 on the mechanics of tumor cells [5]. To fully understand the biomechanical landscape of
116 cancer, it is important to integrate multiple techniques, each tailored to specific research
117 needs. AFM is a widely used method due to its high spatial resolution and ability to measure
118 forces at the nanoscale. It can assess mechanical properties such as Young's modulus,
119 viscosity, surface tension, and adhesion forces in both normal and pathological tissues [6,
120 7]. However, AFM is low-throughput, requires technical expertise, and has limitations
121 related to scan quality and time. MPA involves pulling a cell into a micropipette using
122 negative pressure, with the resulting deformation measured to determine properties such
123 as Young's modulus, surface tension, and intracellular pressure [5, 8]. While inexpensive,
124 MPA has low spatial and temporal resolution, and the quality of the seal between the cell
125 and the pipette can significantly affect the results [9]. Optical tweezers use focused laser
126 beams to manipulate small objects and apply forces in the femtonewton to piconewton
127 range. This technique is ideal for molecular force analysis, as it allows for precise control
128 of low forces. It is useful for studying mechanical compliance, adhesion forces, and surface
129 tension at the molecular level [5]. However, it is inherently low-throughput, as each object
130 is manipulated individually [10]. TFM measures the forces of cells exert on an elastic
131 surface. By analyzing the deformation of the substrate, the forces exerted by the cells can
132 be quantified. This technique does not require chemical perturbations, allowing for natural
133 quantification of cellular stresses. However, it requires accurate imaging of cell-substrate

134 interactions and computational methods to analyze the data [5].

135 Although these methods yield valuable insights into mechanical properties, they are
136 constrained by limitations such as spatial resolution, throughput, and the requirement for
137 direct physical contact with the sample. To overcome these issues, non-contact optical
138 techniques, such as Brillouin microscopy, have emerged. Additionally, ultrasound [11] and
139 magnetic resonance imaging [12] have been used to collect mechanical data non-
140 invasively. While these methods are non-invasive, they have lower spatial resolution
141 compared to other techniques, making them less effective for cellular and subcellular
142 analysis. Furthermore, mechanical properties differ across cell types [13]. For instance,
143 varying collagen/GAG compositions in different cartilage types result in distinct mechanical
144 characteristics [14]. In summary, while current techniques provide valuable information
145 about the mechanical properties of cells and tissues, each has its strengths and limitations.

146 **3. The role of biomechanics in tumor progression**

147 **3.1 Biomechanical modulation of the tumor microenvironment**

148 The tumor microenvironment (TME) composed of interstitial cells and ECM is
149 characterized by a complex interaction between cells. The ECM is primarily composed of
150 intercellular matrix and basement membrane, while the interstitial cells include fibroblasts
151 and immune cells (**Figure 1**). The intercellular matrix, which includes components such as
152 collagen, fibronectins, integrins, laminins, and matrix metalloproteinases (MMPs), plays a
153 crucial role in mediating mechanical properties and is a key element of the mechanical
154 signaling pathway [15]. Unlike normal tissues, tumor tissues have a unique
155 microenvironment characterized by abnormal structures of blood and lymphatic vessels,
156 increased stromal pressure, and a dense interstitial matrix. Recent studies indicate that, in
157 addition to biochemical cues, physical signals from the microenvironment can play a crucial
158 role in influencing cellular behaviors, including growth, metastatic potential, and drug
159 resistance [2]. These physical signals mainly include solid stresses, fluid shear stresses,
160 and indirect mechanical forces (**Figure 1**).

161 Solid stress accumulates in tumors as proliferating cancer cells exert strain on the
162 surrounding structural elements of both tumor and normal tissues [16]. Solid stresses are
163 produced by mechanisms such as cell infiltration, proliferation, matrix deposition, osmotic
164 swelling of glycosaminoglycans like hyaluronic acid (HA), and actomyosin-mediated cell

165 contractions [17]. A portion of this stress arises from reciprocal forces imposed by adjacent
166 normal tissue, while the remainder is stored within the cells and matrix components of the
167 tumor. This residual stress, also known as growth-induced solid stress, persists even after
168 tumor excision and the removal of external forces [16, 18]. Elevated solid stresses within
169 tumors compress blood vessels, reducing blood flow. Concurrently, the excessive
170 deposition and cross-linking of ECM components, such as collagen, lead to ECM
171 remodeling and thus increased stiffness [19]. Therefore, tumors are always appreciably
172 stiffer than normal tissue [20].

173 Interstitial fluid, composed of water and solutes such as soluble carbohydrates and
174 plasma proteins, exists alongside a solid phase formed by the extracellular matrix. The
175 hydrostatic pressure of this interstitial fluid is referred to as interstitial fluid pressure (IFP)
176 or interstitial hydraulic pressure. Fluid shear stresses encompass microvascular and IFP
177 alongside shear forces exerted by blood and lymphatic flow on vessel walls and by
178 interstitial flow on cancer and stromal cells [21]. Elevated IFP, a distinctive feature of solid
179 tumors, results from both solid stress and fluid buildup in the interstitial space [22],
180 potentially influencing tumor cell migration through autocrine C-C chemokine receptor 7
181 signaling [23]. Additionally, IFP in the TME can guide cell movement and promote tumor
182 development. Research by Hyler *et al.* from Virginia Tech - Wake Forest University
183 highlights that even low, continuous fluid shear stress can variably impact adherent
184 epithelial ovarian cancer cells at distinct progression stages [24].

185 The growth and expansion of cells within the TME, especially local pressure variation,
186 also contributed to generating indirect mechanical forces. These forces are mediated by
187 cancer-associated fibroblasts (CAFs) and tumor-associated macrophages (TAMs). They
188 are transmitted to mechanosensors, such as integrins, and play pivotal roles in shaping
189 the mechanical microenvironment of tumors [25].

190 **3.2 Biomechanics and tumor angiogenesis**

191 **3.2.1 The effect of ECM stiffness on tumor angiogenesis**

192 Solid stress from tumor cell growth leads to increased ECM stiffness and
193 compositional changes [26]. ECM stiffening enhances integrin-mediated Rho/ROCK
194 activity and contraction in tumor epithelial and endothelial cells (ECs) [27]. The
195 dysregulation of mechanical force sensing contributes to aberrant behaviors in tumor ECs,

196 resulting in abnormal structure and mechanosensitivity [27]. An *in vitro* study demonstrated
197 that elevating collagen stiffness—without altering the matrix architecture—boosted
198 angiogenic outgrowth and increased vascular branching density in endothelial cell
199 spheroids, thereby facilitating the formation of tumor vascular networks [28].

200 Increased matrix stiffness impacts the function of ECs by impairing vascular barrier
201 integrity, altering VE-Cadherin localization, enhancing permeability, and causing
202 morphological changes in tumor vessels (**Figure 2A**) [29]. Stiffness also disrupts the
203 expression of MS ion channels which regulate tumor angiogenesis. Moreover, the
204 response of ECs to growth factor signaling is closely related to ECM stiffness. In
205 hepatocellular carcinoma (HCC) cells, ECM stiffness up-regulates VEGF expression *via*
206 the integrin β 1/PI3K/Akt pathway and VEGFR2 expression in ECs through the integrin
207 $\alpha_v\beta_5$ /Akt/Sp1 pathway, thus promoting angiogenesis in tumors [30, 31]. Bevacizumab, a
208 well-studied antiangiogenic agent, blocks VEGFA binding to its receptors, thereby inhibiting
209 neovascularization and signal transduction activation [32].

210 **3.2.2 The effect of solid stress on tumor angiogenesis**

211 The accumulation of solid stress also impairs vascular flow in tumors by compressing
212 the more fragile outflow vessels, such as veins and lymphatics, thereby contributing to the
213 increased IFP (**Figure 2B**). Consequently, relieving solid stress can help decompress both
214 blood and lymphatic vessels, leading to improved perfusion and normalization of IFP levels
215 [33]. Recent studies indicate the rising solid stress can reduce vascular patency, resulting
216 in heightened tumor hypoxia [33, 34]. This initiates a harmful feedback loop [34]: tumor
217 growth induces solid stress, which in turn causes hypoxia and prompting collagen
218 remodeling. This remodeling affects angiogenesis and tumor cell invasion, thereby
219 accelerating tumor progression. Solid stresses are primarily generated within matrix
220 components, and many associated complications can be mitigated through drugs that
221 target the degradation of these matrix elements and reduce fibrosis [33]. For instance,
222 losartan, an angiotensin receptor 1 blocker, has been shown to decrease collagen I and
223 hyaluronic acid levels by inhibiting TGF- β signaling [35]. In preclinical models of pancreatic
224 ductal adenocarcinoma (PDAC), losartan alleviates solid stress and decompresses blood

225 vessels, thereby improving the efficacy of chemotherapy and extending overall survival
226 [35].

227 **3.2.3 The effect of fluid stress on tumor angiogenesis**

228 The abnormal blood and lymphatic vessel structures of tumor leads to increased
229 interstitial fluid pressure and heightened permeability of blood vessels, which allows large
230 molecules, such as plasma proteins, to cross the vascular wall and enter the tumor stroma,
231 thereby elevating the osmotic pressure within the interstitium [36]. The rapid growth of
232 tumor cells in a confined space generates internal stress, which compresses intratumoral
233 lymphatic vessels, thus leading to lymphatic dysfunction and fluid retention [37]. Fluid
234 stress within the TME increases viscous and geometric resistance to blood flow, thus
235 resulting in hypoperfusion and insufficient delivery of oxygen and nutrients [29]. This
236 process ultimately results in hypoxia and a decrease in pH levels, and tumor hypoxia
237 subsequently promotes angiogenesis [38, 39]. Elevated IFP in tumors, ranging from 4
238 mmHg to up to 60 mmHg, facilitates the outward flow of interstitial fluid from the tumor core
239 to its periphery.

240 The shear stress within tumor vessels, which is influenced by blood viscosity and
241 shear rate, is impacted by the immature and abnormal structure of these vessels [40]. The
242 endothelial lining of the vascular network demonstrates discontinuities, lacks a complete
243 basement membrane, and shows inadequate pericyte coverage. These structural
244 abnormalities lead to large pores that increase blood plasma leakage into the interstitial
245 space, thereby increasing hemoconcentration and blood viscosity [41]. In tumors, the
246 elevated IFP often surpasses microvascular pressure (MVP), which will restrict perfusion
247 and alter flow dynamics (**Figure 2C-D**). Additionally, tumor vessels may become dilated
248 and tortuous, potentially forming vascular shunts [42]. Solid stress compresses both blood
249 and lymphatic vessels, contributing to increased geometric resistance and significantly
250 reducing blood flow velocity, which can be markedly lower than that in normal vessels [43,
251 44]. This reduced shear stress in intratumoral vessels affects angiogenesis regulation and
252 contributes to abnormalities in the tumor vascular network. Fluid shear stresses specifically
253 influence VEGFR conformational shifts, tubule formation, and barrier integrity, ultimately
254 directing endothelial morphogenesis and sprouting [45].

255 In ECs, transient receptor potential vanilloid 4 serves as a mechanosensor for both

256 shear stress and vascular deformation, affecting tumor angiogenesis and vessel
257 maturation. Shear stress and increased membrane tension also activate G protein-coupled
258 receptors (GPCRs), thus triggering angiogenesis-related signaling pathways such as
259 RhoA, PI3K, MAPK, and Akt [46]. Additionally, pharmacological activation or
260 overexpression of transient receptor potential vanilloid 4 can normalize tumor vasculature
261 and inhibit GPCRs, thereby reducing tumor progression and enhancing the effectiveness
262 of cancer therapies. Tyrosine kinase inhibitors like Anlotinib target these pathways,
263 effectively suppressing angiogenesis by blocking critical phosphorylation events within
264 ECs. Consequently, this leads to the suppression of angiogenesis. Tumors experience a
265 combination of mechanical forces that lead to the development of dysfunctional and leaky
266 tumor vasculature characterized by impaired barrier function and endothelial defects [47].
267 The effective and consistent systemic delivery of cancer therapeutics remains a significant
268 challenge in cancer treatment. To improve therapeutic delivery and efficacy, our group
269 previously reviewed the clinical drugs aimed at normalizing tumor vasculature [48],
270 including Sunitinib, Lenvatinib, and Nintedanib, which have been utilized in combination
271 with chemotherapy to enhance the survival rates of cancer patients.

272 **3.3 Biomechanical regulation of tumor metastasis**

273 Tumor metastasis is primarily a mechanical process [49], in which alterations in
274 cellular biophysical properties, matrix rigidity, and the TME play crucial roles in facilitating
275 cancer invasion and dissemination [50]. The mechanical properties of cellular
276 subcomponents are inherently associated with cancer tissues [5]. For instance, in breast
277 cancer, disruptions in the actomyosin and microtubule cytoskeletons result in a disordered
278 network, correlating with softer and more aggressive cancer cells [51]. In ovarian
279 malignancy, reduced actomyosin contractility results in softer malignant cells, enhancing
280 their migratory capability and aggressiveness [52]. The prevailing view is that cancer cells
281 become softer as they acquire greater aggressiveness and revert to a stiffer state when
282 their aggressive behavior is reduced, typically through pharmacological interventions or
283 genetic silencing of oncogenic factors across various cancers [5]. However, it is important
284 to recognize that this pattern is not universal. For instance, studies in pancreatic cancer
285 have observed that tumors can become stiffer as they grow more aggressive due to the
286 formation of an extensive and dense ECM [53, 54]. Therefore, generalizations about

287 changes in tumor stiffness should be made cautiously, given the considerable variability
288 across different cancer types.

289 Tumor growth intensifies solid stress due to increased cellular density and ECM
290 deposition, thus enhancing the invasiveness of cancer cells [15]. At the onset of tumor
291 metastasis, epithelial cells undergo a transition to a mesenchymal phenotype, thereby
292 resulting in reduced cell-cell adhesion. This process enables tumor cells to breach the
293 basement membrane and basal lamina of the primary tumor, ultimately allowing infiltration
294 into the surrounding tumor microenvironment (**Figure 3A**). After entering the tumor
295 microenvironment, metastatic tumor cells sense vascular and lymphatic endothelial cells.
296 Then, tumor cells disrupt endothelial intercellular junctions, thus facilitating their entry into
297 blood and lymphatic vessels (**Figure 3B**), through which they spread *via* the circulatory
298 system to distant organs. Several factors influence metastatic efficiency of tumor cells,
299 including shear forces and vascular architecture. Hydrodynamic shear stress is known to
300 induce the conversion of circulating tumor cells (CTCs) to less rigid cancer stem cells,
301 enhancing their ability to mimic ECs during the metastatic processes of infiltration and
302 extravasation, thereby facilitating tumor metastasis [2]. The shear forces determine how
303 long CTCs stay adhered to the vessel walls in larger vessels, potentially remaining dormant
304 and increasing their chances of extravasation (**Figure 3C**) [15]. Tumor cells increase
305 intracellular pressure to facilitate nuclear passage through constrictions, such as matrix
306 pores and intercellular gaps between endothelial cells [55, 56]. During this process, the
307 reorganization of the cytoskeleton can influence cellular stiffness and cell shape [57], thus
308 influencing the capacity of cell to penetrate complex tumor stroma or vascular walls (**Figure**
309 **3D**). Additionally, maintaining optimal tumor cell stiffness allows the tumor cells to withstand
310 high shear forces in the bloodstream while crossing endothelial junctions without incurring
311 fatal nuclear damage. At the site of vascular extravasation, the MMP secreted by tumor
312 cells can degrade ECM, reduce the solid pressure and resistance around tumor cells, and
313 thus enable tumor cells to pass through the vascular basement membrane and move
314 closer to the implantation site (**Figure 3E**). Upon reaching a favorable site, tumor cells
315 adhere to the inner lining of blood or lymphatic vessels through integrin or other adhesion
316 ligands (**Figure 3F**), thus forming secondary tumors within the lumen or extravasating
317 through the endothelium to establish secondary growths in surrounding tissues (**Figure**

318 **3G).**

319 Scientists are developing therapeutic strategies aimed at inhibiting tumor metastasis
320 through biomechanical regulation. Paclitaxel and vincristine are commonly used
321 therapeutic drugs for tumors (including ovarian, breast, and brain tumors) in clinical
322 practice, based on the mechanical mechanisms of stable or depolymerized microtubules
323 (MT), indicating that the clinical application of biomechanical therapy is becoming mature
324 [58, 59]. As our understanding of biomechanical influences deepens, it is anticipated that
325 a greater array of novel anti-tumor drugs will be integrated into clinical practice to improve
326 the management of tumor metastasis.

327 ***3.4 Biomechanical regulation of tumor drug resistance***

328 Growing evidence indicates that the biomechanical microenvironment and the
329 physical properties of tumor cells are crucial in promoting tumor resistance [60]. For
330 instance, the composition, stiffness, and structure of the ECM are critical determinants
331 influencing the response of cancer cells to therapeutic agents [61]. Adhesion of cancer
332 cells to ECM components, such as collagen and fibronectin, or their growth in a stiff matrix,
333 drives resistance to chemotherapy. When the ECM is stiff, ATP-binding cassette (ABC)
334 transporters are less active and less effective at removing drugs from cells. Conversely,
335 when the ECM is more compliant or soft, ABC transporters are more active, which can
336 enhance drug clearance [62]. Hypoxia and acidity are key characteristics of tumor
337 metabolism that greatly enhance tumor resistance to radiation therapy, chemotherapy, and
338 other treatment modalities [63]. In the TME, hypoxia triggers stiffening of the ECM, further
339 enhancing the drug resistance of tumor cells [64, 65].

340 High interstitial pressure and shear stress within the tumor can alter the morphology
341 and behavior of tumor cells, thus enhancing the remodeling and adhesion capabilities of
342 the cytoskeleton [5]. This mechanical stress can activate multiple signaling pathways,
343 including yes-associated protein (YAP)/transcriptional coactivator with PDZ-binding motif
344 (TAZ), which promote the survival and resistance of tumor cells [66]. Further, the stiffness
345 of the ECM can impede drug penetration into tumors. Studies on breast cancer cells have
346 demonstrated that their response to chemotherapeutic agents significantly varies with
347 substrate stiffness. While the cells cultured on substrates with increased rigidity have been
348 observed to demonstrate a heightened resistance to specific chemotherapeutic agents [67].

349 This resistance is further supported by the high deposition of collagen proteins, which bind
350 to proteoglycans and stabilize ECM components, thus enhancing its stiffness (**Figure 4A**).
351 Notably, treatment with collagenase has been shown to increase IgG diffusion to tumor
352 sites in penetration-resistant tumors [68]. In all, targeting the stiffness of the ECM could
353 offer new strategies to overcome chemoresistance.

354 Other evidence indicates that ECM stiffness modulates the activation of YAP, which is
355 significantly associated with drug resistance across various human cancer cell lines [66,
356 69]. Upon activation, the nuclear translocation of YAP may contribute to drug resistance by
357 regulating anti-apoptotic gene transcription and interacting with the MAPK and PI3K-AKT
358 signaling pathways [66]. CAFs are primary contributors to ECM stiffness during tumor
359 development. Within the TME, CAFs interact with cancer and immune cells, reshaping the
360 ECM to promote tumor progression (**Figure 4B**) [70]. Additionally, CAFs influence cancer
361 cell behavior and response to treatments through ECM remodeling [71].

362 In addition to the tumor microenvironment, drug-resistant tumor cells exhibit distinct
363 lipid metabolism from that of sensitive cells to reduce the damage caused by chemotherapy,
364 thus resulting in different lipid compositions and membrane characteristics [72]. For
365 example, drug-resistant ovarian cancer cells increase the uptake of extracellular
366 cholesterol [73], and enhance cholesterol synthesis [74], thereby elevating cholesterol
367 levels in their membranes. The high cholesterol content in the membranes of drug-resistant
368 ovarian cancer cells leads to thicker and more rigid membranes, resulting in reduced drug
369 permeability, which is one of the significant reasons for the development of drug resistance
370 in tumor cells (**Figure 4C**) [75, 76]. Moreover, the increased cholesterol and sphingolipid
371 content in the lipid rafts of drug-resistant tumor cells enhances the expression, recycling,
372 and bioactivity of multidrug resistance transporters (such as ABC transporters)
373 concentrated in these regions [77, 78]. Cholesterol can alter the rigidity and fluidity of lipid
374 rafts, thereby modifying the spatial conformation of multidrug resistance proteins within
375 their domains, making it easier for these proteins to bind and transport intracellular
376 chemotherapy drugs (**Figure 4D**) [79]. Maintaining high levels of cholesterol within the lipid
377 rafts of resistant cells is crucial for supporting the bioactivity of P-glycoprotein located
378 therein [80]. A study has shown that depleting cholesterol-enriched sphingolipid lipid rafts
379 with small-molecule drugs can successfully reverse tumor resistance [81]. In general,

380 targeting the mechanical properties of tumor cells offers a promising strategy to overcome
381 drug resistance.

382

383 **4. Decoding biomechanical signaling mechanisms of cancer cells**

384 **4.1 Tumor cellular mechanosensors**

385 The study of tumor cellular mechanosensors opens a crucial pathway for
386 understanding the intricate mechanisms through which cancer cells perceive and react to
387 biomechanical forces within their microenvironment. Tumor cellular mechanosensors
388 primarily consist of the glycocalyx, primary cilium, cytoskeleton, and nucleus. Glycocalyx
389 is the sugar and glycoprotein covering layer on the outside of the cell membrane. Primary
390 cilium is a tiny protrusion on the cell membrane, and the cell membrane is the base of
391 glycocalyx and primary cilium. The cytoskeleton is intricately linked to the cell membrane
392 and the basal body of the primary cilium, which offers essential structural support for both.
393 It not only senses mechanical signals but also plays an important role in transmitting these
394 signals.

395 **4.1.1 Glycocalyx**

396 Glycoproteins and proteoglycans represent the predominant glycan categories within
397 the glycocalyx (GCX) [82]. Proteoglycans are composed of core proteins attached to
398 glycosaminoglycan (GAG) chains, including heparan sulfate (HS) and HA, as well as
399 sialoglycoproteins. The GCX, interfacing directly with the ECM, plays an essential role in
400 mediating integrin adhesions to the ECM and in responding mechanically to environmental
401 stiffness (**Figure 5A**) [83]. Furthermore, the specific composition and size of the GCX
402 influence the extent of mechanosensing experienced by cell-bound integrins upon
403 contacting the ECM [84]. Notably, bulky cancer-associated glycoproteins like MUC1 are
404 known to facilitate integrin clustering and enhance mechanosensing capabilities [85].
405 Research indicated that overexpressing MUC13 in Panc-1 cells typically reduced their
406 modulus and diminishes adhesion. Conversely, knocking down MUC13 in HPAF-II cells
407 leads to increased modulus and enhanced adhesion [86]. Therefore, it is speculated that
408 tumor cell-cell adhesion can be enhanced and invasiveness can be reduced by reducing
409 the volume or directly knockdown of the expression of GCX.

410 The GCX on cancer cells is notably dense, aiding in integrin clustering, growth factor

411 signaling, and mechanotransduction of elevated interstitial flow shear stress within tumors.
412 This process subsequently promotes release of MMPs, which will enhance cell motility and
413 metastasis [82]. Research by Qazi *et al.* from City University of New York indicated that
414 such interstitial flow notably increased migration in SN12L1 cells (high metastatic potential)
415 of human kidney carcinoma lines, unlike in SN12C cells (low metastatic potential) [87].
416 Specifically, the expression of MMP-1, MMP-2, CD44, and α 3 integrin were upregulated by
417 interstitial flow in SN12L1 cells, while it remained unchanged in SN12C cells. Moreover,
418 enzymatic cleavage of GCX components, such as HS or HA, inhibited flow-induced
419 migration and MMP expression in SN12L1 cells. This suggests that the GCX in cancer
420 cells serves as a mechanosensor for interstitial flow shear stress, coordinating the
421 expression of MMP-1, MMP-2, CD44, and α 3 integrin to control cell migration and
422 metastasis. Additionally, 4-Methylumbelliferone inhibits HA synthesis by downregulating
423 HA receptors and the phosphatidylinositol 3-kinase/CD44 complex [88]. The anti-CD44
424 monoclonal antibody A6 has been shown to inhibit tumor cell migration, invasion, and
425 metastasis by blocking CD44-mediated signaling pathways [89].

426 Understanding the MS and transductive functions of the GCX on tumor cells have
427 paved the way for innovative cancer therapeutic strategies. First, modulating GCX
428 mechanotransduction will block GCX-mediated adhesive interactions, which will reduce
429 tumor cell extravasation, potentially halting metastasis and improving patient survival rates
430 [90]. Second, reducing the thickness of the GCX enhances immune recognition by natural
431 killer cells, which can be achieved by degrading the GCX, thereby augmenting the
432 cytotoxicity of these immune cells [91]. Lastly, editing the composition of the GCX through
433 self-executed feedback loops presents a novel and manageable approach to cancer
434 treatment [92].

435 **4.1.2 Primary cilia**

436 Primary cilia (PC) consist of a microtubule-based core, called the axoneme, which
437 extends from a specialized centriole known as the basal body and is enclosed by a lipid
438 bilayer continuous with the cell membrane (**Figure 5B**). Despite their small size, PC
439 constitutes approximately 1/200 total surface area of the cell. The PC are critical for both
440 development and homeostasis of the body. These structures are densely packed with
441 receptors, ion channels, and downstream signaling molecules critical for numerous

442 pathways, such as Hedgehog and GPCR signaling. The absence of this antenna-like
443 structure results in improper signaling activation. Consequently, mutations that disrupt the
444 assembly, structure, or function of cilia impair the transmission of mechanical signals,
445 resulting in ciliopathies—a diverse group of over 30 human diseases and syndromes
446 affecting various organs and tissues, including the eye, heart, kidney, brain, liver, and bone
447 [93].

448 Under fluid flow stimulation, PC deflect, transmitting mechanical strains *via* the
449 cytoskeleton to critical cytoplasmic organelles like the Golgi complex, which governs the
450 response of cell to mechanical stimuli. Modifying the length and rigidity of PC can influence
451 this cellular mechanosensitivity [94]. Notably, primary cilia are frequently absent in various
452 cancers [95], including glioblastoma, melanoma, pancreatic, prostate, ovarian, colon,
453 breast, medulloblastoma, and renal cancers, as opposed to their presence in normal tissue
454 [96]. In cholangiocarcinoma cases without primary cilia, inhibiting histone deacetylase 6, a
455 protein involved in cilia disassembly, has been shown to restore cilia formation and
456 suppress tumor growth [97].

457 Approximately 25% of tumors in patients with PDAC exhibit PC. The presence of PC
458 is associated with an increased incidence of lymph node metastasis [98]. Research by
459 Martínez-Hernández et al. from Spain demonstrated a marked elevation in PC levels in
460 pituitary neuroendocrine tumors (PitNETs), which was associated with increased tumor
461 invasiveness and higher recurrence rates[99]. Additionally, molecular analysis revealed the
462 dysregulation of 123 cilia-associated genes, including doublecortin domain containing
463 protein 2, syntaxin-3, and centriolar coiled-coil protein 110 in PitNETs. Moreover, an
464 increase in both the formation and length of primary cilia has been observed in cancer cells
465 that exhibit resistance to anti-cancer drug kinase inhibitors [100]. Thus, regarding a clear
466 link between PC and tumorigenesis, the impact of PC on cancer progression may differ
467 depending on the specific type and stage of the cancer. Regulating the expression and
468 mechanical properties of PC holds the potential to unveil new therapeutic strategies, given
469 their pivotal role in biomechanical signal transduction and resistance to chemotherapy in
470 cancer cells. Future investigations might focus on accurately modulating these structures
471 to enhance therapeutic outcomes and curtail tumor progression.

472 **4.1.3 Cytoskeleton**

473 The primary components of cytoskeleton include MTs, actin filaments, and
474 intermediate filaments. It not only senses and transduces mechanical stress but is also
475 influenced by external forces from the ECM (**Figure 5C**) [101]. When mechanical forces
476 are applied to cancer cells, actin filaments act as mechanosensors that detect these forces
477 [102]. These filaments generate contractile forces through interactions with myosin II and
478 through polymerization, which drives the forward movement of the plasma membrane [103].
479 MTs are essential in aligning chromosomes and organizing the spindle in response to
480 mechanical forces during mitosis [104]. In tumor cell migration, MTs facilitate pseudopodia
481 formation, which reacts to mechanical signals from the TME [105]. Intermediate filaments,
482 recognized for their stability and durability, are critical in sensing the magnitude and
483 direction of mechanical forces encountered by cancer cells. As tumors progress, the
484 cytoskeleton undergoes continual remodeling, allowing tumor cells to develop distinctive
485 mechanical properties and adapt to the dynamic shifts within their microenvironment [106].
486 During tumor progression, tumor cells actively remodel their cytoskeletal structures and
487 decrease cellular stiffness [107]. As tumor cells enter and exit the vascular system, they
488 experience significant shape alterations facilitated by cytoskeletal remodeling, which
489 enable them to traverse endothelial cell-cell junctions [108]. Research by Liu *et al.* from
490 Chengdu Medical College has shown that low shear stress markedly enhances both the
491 percentage and length of filopodia, which are vital for cancer cell mobility and can trigger
492 migration[109]. However, shear stress may also influence tumor progression through
493 synergistic interactions with chemical factors like chemokines or growth factors, and
494 mechanical factors such as matrix stiffness. Further research is needed to elucidate the
495 complex tumor microenvironment's impact. Recent findings indicate that the cytoskeletal
496 structure and biophysical characteristics of breast cancer subgroups are linked to their
497 metastatic preference, regarding the gene expression profiles and mechanoadaptation
498 capacities [110]. Therefore, by increasing the shear stress and inhibiting Cdc42, filopodia
499 is greatly reduced, thereby reducing tumor metastasis.

500 Modulating the mechanical properties of the cytoskeleton is a promising strategy for
501 tumor therapy. A research obstacle is to develop equipments capable of measuring and
502 applying forces. Future studies should focus on integrating mechanotransduction research
503 with therapeutic interventions by identifying key molecules that promote cell health or treat

504 diseased cells. Additionally, it is important to understand how cellular mechanosensors
505 interact with the tumor microenvironment to activate cytoskeletal movements. This will
506 require a multidisciplinary approach to model mechano-responses and develop treatments
507 that can reverse cancer pathologies.

508 **4.1.4 Cell nucleus**

509 The nucleus, notable for being both the largest and stiffest organelle, is also highly
510 dynamic, capable of sensing external mechanical cues and adapting rapidly [111, 112]. The
511 nucleus plays an integral role in mechanoregulation, which encompasses both
512 mechanosensing and mechanotransduction processes (**Figure 5D**). Surface
513 mechanoreceptors detect these cues and transmit signals to the nucleus, influencing
514 cytoskeletal integrity and tension. This leads to adjustments in gene expression related to
515 mechanical stimulation [113]. Changes in nuclear mechanics, such as those induced by
516 the ECM, can influence the morphology of nucleus and localization of transcription factors
517 [114]. Cellular adaptations to matrix tension involve alterations in lamin A phosphorylation
518 and nuclear positioning, which are regulated *via* the mechanotransduction pathways of
519 YAP and retinoic acid receptor (RAR), ensuring cytoskeletal equilibrium [45]. Cells adapt
520 to matrix tension by modifying lamin A phosphorylation and nuclear positioning, and
521 maintain cytoskeletal balance through the mechanosignaling routes of YAP and RAR [114].

522 Cell spreading and nuclear stretching activate MS calcium channels on the nuclear
523 membrane, leading to an increase in nuclear calcium levels. This increase causes elevated
524 levels of the transcription factor CREB, which is vital for regulating gene transcription,
525 protein import, apoptosis, and subsequent mechanosignaling processes [115, 116]. The
526 phosphorylation of Lamin A/C and Emerin within the nucleus responds to mechanical
527 stimulation by altering nuclear stiffness and nucleo-cytoskeletal coupling [114]. Further,
528 changes in chromatin organization, condensation, and modification are influenced by the
529 actin cytoskeleton and the linker of nucleoskeleton and cytoskeleton complex [117, 118].

530 Cytoskeletal contraction also triggers adenosine triphosphate (ATP) release and
531 calcium signaling, which facilitate the nuclear import and activation of histone modifiers,
532 such as enhancer of zeste homolog 2 and histone deacetylase [117, 118]. These processes
533 drive cancer-related gene silencing and transcriptional regulation through alterations in
534 histone methylation [119] and acetylation [120]. Furthermore, polymerization of nuclear

535 actin adjusts nuclear structure and transcription factor functionality, influencing gene
536 expression through enhanced nuclear transport mechanisms [121]. Softer nuclei,
537 characterized by reduced levels of lamin A/C, are more susceptible to rupture and
538 subsequent DNA damage during migration [122]. In contrast, cells with stiffer nuclei,
539 induced by progerin, also exhibit increased DNA damage [123]. This paradox highlights
540 the complex role of nuclear mechanics in cellular health. The research conducted by Nava
541 *et al.* from University of Helsinki demonstrated that mechanical stretching of the nucleus
542 induced a calcium-dependent softening mediated by chromatin alterations, and inability to
543 initiate the nuclear MS response led to DNA damage [124]. Subsequent DNA damage
544 response reorganizes the nucleus, altering chromatin structure to facilitate more efficient
545 DNA repair, which may inadvertently contribute to chemotherapeutic resistance [125].

546 **4.2 Mechanosignaling proteins**

547 In addition to cellular mechanosensors, a range of mechanical signals are perceived
548 and relayed to cells *via* the activation of surface mechanosignaling proteins like integrins
549 [83], YAP/TAZ [126], transient receptor potential (TRP) ion channels [127], GPCRs [128],
550 and Piezo channels [129]. The mechanosignaling proteins transmit these cues to cellular
551 internal components, thus influencing the behavior of tumor cells.

552 **4.2.1 Integrins**

553 Integrins, which are transmembrane proteins, bind to diverse ECM proteins and play
554 a pivotal role in detecting changes in the extracellular environment (**Figure 5E**). These
555 proteins are critical for cell adhesion and signal transduction. They facilitate the detection
556 of the mechanical properties within the ECM and relay these signals to focal adhesion
557 kinase (FAK). This interaction strengthens focal adhesions and triggers subsequent
558 intracellular signaling pathways [130]. In the TME, FAK influences both cancer and stromal
559 cells, enhancing tumor progression and metastatic potential [131].

560 Integrin-mediated adhesions engage with the ECM and respond to its rigidity,
561 consequently influencing cellular activities including motility and migration [132]. Integrin
562 interactions with specific ECM components trigger outside-in signaling that regulates the
563 cytoskeleton. Concurrently, mechanical forces generated by the cytoskeleton are
564 transmitted back to integrin-ECM interactions, promoting cancer metastasis [133]. Several
565 clinical studies have linked high integrin expression to poor cancer survival [106]. Integrin-

566 mediated mechanotransduction reciprocally affects the mechanical properties of the TME.
567 In non-small cell lung carcinoma cells, the absence of integrin $\alpha 11$ is associated with
568 reduced collagen reorganization and lower tissue stiffness, which in turn inhibits cell growth
569 and metastatic potential [134]. This phenomenon highlights the pivotal role of stromal
570 integrin $\alpha 11$ expression in collagen cross-linking. In colon cancer cells, integrins are
571 responsive to mechanical stimuli, particularly shear stress, which leads to the
572 downregulation of integrin $\beta 1$ -FAK signaling, subsequently enhancing the cytotoxic effects
573 of radiation [135]. The deregulation of integrin signaling, facilitated by alterations in the
574 ECM and integrin diversity, allows cancer cells to rapid cell proliferation, invade tissues,
575 and adapt to different environments [136]. As a result of dynamic remodeling of the ECM,
576 tumor cells change in density, hardness, or tissue composition. For instance, the
577 progression of breast cancer is associated with elevated mechanosignaling and increased
578 tissue birefringence, suggesting that ECM hardness promotes malignancy and increases
579 tumor aggressiveness [137]. Moreover, hypoxia-inducible factor 1 upregulates the
580 expression of lysyl oxidase which enhances the crosslinking of collagen fibers. This
581 process increases the stiffness of the TME, which in turn enhances integrin-mediated
582 signaling and promotes cell proliferation [138].

583 During the early stages of tumorigenesis, neoplastic conversion significantly impacts
584 the expression levels of specific integrins, resulting in changes to the integrin profile on
585 cancer cells. It triggers modifications in integrin signaling pathways that facilitate the
586 advancement of neoplastic transformation [139]. Oncogenic signaling plays an important
587 role in driving these alterations. For example, in terms of ovarian cancer, mutant p53
588 operates via integrin $\alpha 5\beta 1$ to enhance the expression of the epithelial-mesenchymal
589 transition (EMT) transcription factor TWIST1. This process promotes the formation of tumor
590 cell clusters that penetrate the mesothelium and subsequently proliferate into peritoneal
591 tumors [140]. However, certain integrins, like $\alpha 2\beta 1$, may impede tumor progression,
592 highlighting the complex and variable roles of integrins in cancer [141]. Given their
593 overlapping functions in adhesion and signaling, it is challenging to develop specific
594 inhibitors and sensitive biomarkers. Over the past 30 years, many drug discovery projects
595 and clinical studies have focused on integrins. However, the approved anti-cancer drugs
596 targeting integrins are limited [142]. Therefore, a comprehensive investigation into integrin

597 dependency across various cancer types, coupled with biomarker development using
598 genetically engineered and patient-derived xenograft models, is essential for advancing
599 integrin-targeted cancer therapies.

600 **4.2.2 Cadherins**

601 Cadherins, such as E-, VE-, N-, R-, P-, and K-cadherin, are transmembrane proteins
602 that function as cell-cell interaction receptors and enable calcium-dependent adhesion
603 [143]. In tumors, cadherins act as critical mechanosensors that detect and convey
604 mechanical signals from neighboring cells (**Figure 5F**). The cadherin cytodomain connects
605 to the actin cytoskeleton through β -catenin and α -catenin, thereby regulating
606 mechanotransduction [144]. Among the classical family of cadherins, E-cadherin plays a
607 central role as a mechanosensor by both sensing and facilitating the transmission of
608 mechanical forces [145]. The force transduction mediated by E-cadherin influences various
609 cellular functions. It activates signaling *via* the epidermal growth factor receptor (EGFR),
610 which governs local cytoskeletal restructuring and promotes cellular proliferation [146]. E-
611 cadherin is identified as a tumor suppressor protein, and its decreased expression
612 associated with the EMT is a common occurrence in the process of tumor metastasis. By
613 enhancing E-cadherin expression, α -solanine (a glycoalkaloid extract of *Solanum nigrum*
614 Linn) inhibited endothelial cell transformation and exhibited potent anti-carcinogenic
615 properties [147].

616 Moreover, the internalization of E-cadherin in response to blood flow may represent
617 an adaptive metastatic mechanism that enhances cellular motility and invasion [148].
618 Concurrently, a stiffer ECM elevates N-cadherin expression on endothelial cells, enhancing
619 their interaction with tumor cells and vascular endothelium to facilitate metastasis [149].
620 Additionally, E-cadherin affects the activity of transcriptional coregulators such as catenins
621 and YAP. Under biaxial mechanical stretch conditions, YAP and β -catenin, which are
622 components of the cadherin complex, promote cell cycle progression in an E-cadherin-
623 dependent manner [150]. The modulation of actin cytoskeleton rigidity influences the
624 interaction between APC and β -catenin, thereby affecting the localization of β -catenin
625 within the nucleus or cytoplasm. The suppression of β -catenin-mediated transcription
626 impeded the progression of the cell cycle from the G1 phase to the S phase [150]. Moreover,
627 the cadherin-mediated mechanical force transmission, especially *via* the N/E-cadherin

628 complex, is key to tumor cell migration and invasion. Inhibiting this complex can reduce
629 interactions between mesenchymal-like and epithelial-like cancer cells, thus decreasing
630 tumor aggressiveness [151]. Overall, the cell-cell interaction mediated by cadherin is
631 crucial for the migration, survival, and proliferation of cancer cells. However, the specific
632 impact of cadherin-driven mechanotransduction on tumor progression *in vivo* warrants
633 further exploration.

634 **4.2.3 Mechanosensitive ion channels**

635 During tumor progression, mechanical cues activated by MS ion channels influence
636 both the cancer cells and their surrounding microenvironment. These mechanical signals
637 are converted into cellular responses, including proliferation (**Figure 5G**) [152]. MS ion
638 channels, including epithelial sodium channels, TRP channels, two-pore domain potassium
639 channels, and Piezo channels, convert mechanical stimuli at the cell membrane into
640 biochemical signals *via* mechanotransduction [5, 153].

641 Piezo1 and Piezo2, the primary mechanosensors in mammals, facilitate cellular
642 adaptations to mechanical forces [153]. Their upregulation is linked to increased
643 proliferation, migration, and invasion in tumor cells, suggesting their potential as
644 therapeutic targets in cancer [154, 155]. Changes in the matrix microenvironment may
645 result in the overexpression of certain MS ion channels, including Piezo1. Specifically, the
646 study by Chen *et al.* from hospital for sick children in Canada demonstrated that Piezo1
647 activation could initiate integrin-FAK signaling, influence ECM composition, and contribute
648 to tissue stiffening. Meanwhile, the stiffer environment increased the expression of Piezo1,
649 inducing glioma aggression [156]. Thus, targeting Piezo1 offers a potential strategy to
650 interrupt the harmful feedback loop between the mechanotransduction of tumor and
651 abnormal tissue mechanics [156]. Mechanical stimuli, including stretch and compression,
652 activate Piezo1 and its associated signaling pathways, such as the Akt/mTOR pathway in
653 prostate cancer [106], thereby promoting cell cycle progression and enhancing tumor cell
654 invasion as well as matrix degradation. Additionally, Piezo1-mediated calcium influx
655 induced by circulatory shear stress increases susceptibility of cancer cells towards TRAIL-
656 induced apoptosis [157], underscoring the potential of targeting Piezo1/2 in cancer therapy.

657 As cationic channels, TRP proteins could be activated by physicochemical stimuli to
658 regulate diverse sensory capabilities which are associated with various cancers[158].

659 Among them, transient receptor potential melastatin 7 (TRPM7) is a MS TRP ion channel,
660 whose expression is notably altered in various cancers [159]. High TRPM7 levels are linked
661 to EMT pathway activation and are associated with reduced disease-free and overall
662 survival in ovarian cancer cells [160]. Additionally, TRPM7 is essential for activating Notch
663 and JAK/STAT3 pathways in glioblastoma, increasing the levels of cancer stem cell marker
664 ALDH1 [159]. Above all, these insights underscore the potential of MS ion channels as key
665 targets in the development of novel cancer therapies, leveraging their MS properties to
666 counteract tumor progression.

667 **4.2.4 G protein-coupled receptors**

668 GPCRs constitute the largest family of membrane receptors, characterized by diverse
669 intracellular signaling properties that originate from the activity of G-protein subunits [161].
670 GPCRs have been postulated independently to mediate mechanotransduction [162] and
671 to facilitate changes in cell shape (**Figure 5H**) [163]. Recently, the function of GPCRs as
672 mechanosensors in cancer cells has been progressively demonstrated [106]. Yang *et al.*
673 [164] from first affiliated hospital of Xi'an Jiaotong University showed a member of the
674 GPCR family, C-X-C chemokine receptor type 4 (CXCR4), acted as a crucial intracellular
675 signal transducer to regulate mechano-sensitive cellular activities through YAP signaling
676 pathway mediated by ubiquitin domain-containing protein 1. Their study demonstrated that
677 the expression of CXCR4 was significantly upregulated in HCC cells as matrix stiffness
678 increased, driving cell growth, EMT, and cancer cell stemness. Notably, luteolin, a natural
679 compound, was found to suppress the effects induced by matrix stiffness and block the
680 CXCR4-driven YAP signaling pathway within HCC cells [164].

681 Evidence suggested that targeting GPCR function could effectively slow or prevent
682 the progression and metastasis of various cancers [165]. GPCRs, such as those
683 responsive to chemokines, thrombin, and neuropeptides, represent promising targets for
684 pharmacological interventions in cancer prevention and therapy [165]. Studies by Liu *et al.*
685 from Kunming University of Science and Technology have demonstrated that GRPR-
686 specific inhibitors could significantly reduce tumor growth and angiogenesis, highlighting
687 their potential in clinical cancer management [166]. Despite GPCRs being crucial drug
688 targets, their exploitation as cancer targets is limited, with few anti-cancer compounds that
689 modulate GPCR-mediated signaling currently in clinical use [166]. Maraviroc, an FDA-

690 approved antagonist of the C-C chemokine receptor 5 (CCR5), showcases the potential of
691 small molecules in inhibiting GPCRs [167, 168]. A phase I trial confirmed the anti-tumor
692 effects of a CCR5 antagonist in patients with advanced, refractory colorectal cancer and
693 liver metastases [169]. In general, GPCRs play a crucial role in transducing mechanical
694 signals within tumor cells. Moreover, combinatorial immunotherapies that target GPCRs
695 are emerging with promising effects for cancer treatment, highlighting the potential of
696 GPCRs in mechanotransduction and cancer cell behavior [170].

697 **4.2.5 YAP/TAZ**

698 YAP and the transcriptional coactivator TAZ function as mechanosensors and
699 mechanotransducers, responding to ECM stiffness, cell morphology, and cytoskeletal
700 tension, which are essential for nuclear localization (**Figure 5I**) [171]. YAP/TAZ activity is
701 closely linked to the structure of the actin cytoskeleton, which reinforces membrane-
702 cytoskeleton integrity and supports cancer cell viability during metastasis [172]. These
703 proteins are central to tumor morphogenesis by reshaping the TME to promote growth and
704 evade immune surveillance, influencing not only tumor cells but also surrounding
705 fibroblasts, immune, and endothelial cells [69].

706 YAP/TAZ are frequently deregulated in cancer due to alterations in
707 mechanotransduction, inflammation, oncogenic signaling, and inhibition of the Hippo
708 pathway [173]. This deregulation enhances force transmission between oncogene-
709 expressing cells and the ECM, facilitating tumorigenesis through YAP/TAZ
710 mechanotransduction [174]. YAP additionally stimulates the expression of cytoskeletal
711 regulators, which allows fibroblasts to increase matrix stiffness and facilitate cancer cell
712 invasion [175].

713 Targeting YAP/TAZ could be a viable cancer treatment strategy. IAG933, an inhibitor
714 developed by Novartis targeting YAP/TAZ-mediated transcription, is currently undergoing
715 a phase I clinical trial for tumors with YAP/TAZ gene fusions (NCT04857372) [69]. Similarly,
716 VT3989 from Vivace Therapeutics is undergoing a Phase I trial for solid tumors and
717 mesotheliomas with NF2 mutations (NCT04665206) [69]. Drugs like dasatinib, targeting
718 SRC family members, also show potential in inhibiting YAP/TAZ activity in both laboratory
719 and clinical settings [176]. However, the clinical efficacy of these treatments has been
720 variable, indicating a need for continued research into effective YAP/TAZ inhibitors [176].

721 While research is still in its early stages, these studies are expected to be crucial for
722 developing new anti-tumor drugs and treatment strategies in the future.

723 **4.2.6 Other mechanosignaling proteins**

724 Rho GTPases, a family of small G proteins, are essential regulators of cytoskeletal
725 dynamics, cell polarity, motility, vesicular transport, cell cycle progression, differentiation,
726 and gene expression [177]. Activation of growth factor receptors and integrins promotes
727 the exchange of guanosine diphosphate (GDP) for guanosine triphosphate (GTP) on Rho
728 proteins, allowing GTP-bound Rho proteins to interact with effectors that regulate their
729 activity and localization [178]. In humans, around 20 kinds of Rho GTPases have been
730 identified, with RhoA, Rac, and Cdc42 being the most extensively studied. These proteins
731 are key in remodeling actin-rich cytoskeletal structures and regulating cell contractility,
732 influencing many cellular processes [179]. In cancer, Rho GTPases are typically
733 overexpressed [177]. The overexpression of active RhoA, RAC1 [180], or Cdc42 [181] in
734 rodent fibroblasts enhances anchorage-independent growth and tumorigenesis.
735 Furthermore, effectors such as Rho-associated coiled-coil-containing protein kinase
736 (ROCK) and p21-activated kinases (PAKs) play an important role in cellular transformation;
737 elevated levels of ROCK2 have been associated with high-risk neuroblastoma and adverse
738 patient outcomes, indicating that ROCK inhibitors could offer therapeutic benefits [182].
739 Targeting these regulators, either alone or combined with MAPK or SRC therapies, may
740 offer effective treatment options. Recently, small-molecule inhibitors of Rho GTPases have
741 shown promise *in vitro* and *in vivo* [183]. For example, AZA1, a specific inhibitor of
742 Cdc42/RAC1, effectively suppresses prostate cancer growth *in vivo* and improves survival
743 in mouse models [184].

744 Research has demonstrated that forces applied to the cell surface can transmit to
745 chromatin *via* the cytoskeleton and nuclear proteins, leading to chromatin stretching and
746 activation of gene expression [15]. Nuclear proteins primarily regulate gene expression,
747 translation, and related processes [185]. Abnormal expression of certain nuclear proteins
748 is associated with tumorigenesis, drug resistance, and metastasis [186, 187]. Notably,
749 mutations in these proteins can affect nuclear mechanics and cytoskeletal organization,
750 influencing various cellular functions [188]. For example, mutations in nuclear envelope
751 proteins disrupt mechanotransduction signaling and force transmission [189]. Poh *et al.*

752 from University of Illinois at Urbana-Champaign [190] found that applying excessive force
753 led to rapid and irreversible dissociation of survival of motor neuron from coilin in the Cajal
754 body of HeLa nuclei [190]. This dissociation was sensitive to substrate stiffness, suggesting
755 that sufficient cytoskeletal tension is essential for transmitting forces to the nucleus and
756 inducing deformations [191]. Since Cajal body interact directly with chromatin, these results
757 indicate that force-induced dissociation of nuclear proteins can alter gene expression.
758 Further studies are necessary to determine the functional consequences and longevity of
759 these transcriptional changes [192].

760 In general, mechanosignaling proteins are being recognized for their pivotal roles in
761 the occurrence and progression of tumors [5]. Additionally, these proteins that influence
762 the mechanosensitivity and mechanotransduction of cancer cells represent potential
763 therapeutic targets. Numerous agents that block mechanosignal transduction have already
764 entered clinical trials (**Table 1**). As research advances, biomechanical regulation strategies
765 are expected to pioneer new avenues for cancer therapy.

766

767 ***5. Biomechanical regulation tumor nanotherapeutic strategies***

768 Nanotechnologies offer transformative potential in biomechanical regulation for tumor
769 therapy by targeting the mechanical characteristics of TME and cancer cells. Such
770 technologies enable precise control over cellular biomechanics, which is crucial for
771 developing effective therapies. For example, the unique enhanced permeability and
772 retention (EPR) effect of tumor tissue can retain more nano-sized systems, thereby
773 achieving passive drug enrichment in the tumor site; targeted drug delivery systems can
774 selectively interact with primary cilia or cytoskeletal components, thus enhancing the
775 therapeutic efficacy on tumor; advances in molecular self-assembly technologies and
776 mechanical modulation of the ECM hold promise for disrupting tumor progression and
777 improving treatment outcomes [193]. In this context, we delineate innovative therapeutic
778 approaches leveraging nanotechnology to modulate the perception and transduction of
779 tumor biomechanical signals. These strategies are designated as biomechanical regulation
780 tumor nanotherapeutic strategies (**Table 2**).

781 ***5.1 Interfering primary ciliary biomechanical function***

782 Primary cilia play a role in sensing chemical and mechanical signals. Compounds that

783 regulate cilia length can enhance mechanosensitivity [194]. In glioblastoma, primary cilia
784 formation is reduced. Loskutov et al. from Virginia University School of Medicine [195]
785 reported that lysophosphatidic acid receptor 1 (LPAR1) accumulates in cilia, where it binds
786 lysophosphatidic acid (LPA) to promote cell proliferation. When cilia are lost, LPAR1 moves
787 to the plasma membrane, driving tumor cell proliferation. The small molecule Ki16425
788 inhibits LPA signaling and suppresses glioblastoma growth. In a mouse model, Ki16425-
789 loaded nanoplasts significantly reduced tumor progression, suggesting a potential
790 therapeutic strategy for glioblastoma.

791 Primary cilia are cell organelles that expose themselves to the extracellular lumen,
792 providing an important access to target the cilia. With a diameter of about 250 nm, primary
793 cilia make nano-sized particles promising vehicles for drug delivery. In a study, Pala *et al.*
794 from University of California Irvine reported a kind of cilia-targeted (CT) nanoparticles for
795 the precise delivery of the therapeutic drug (fenoldopam), termed CT-Fe₂O₃-NPs (**Figure**
796 **6A-B**) [196]. High-resolution differential interference contrast imaging was used to locate
797 cilia and assess the selectivity and specificity of CT-Fe₂O₃-NPs. Results indicated that both
798 control CT-Fe₂O₃-NPs without fenoldopam (cCT-Fe₂O₃-NPs) and CT-Fe₂O₃-NPs exhibited
799 specific CT delivery; however, only CT-Fe₂O₃-NPs containing fenoldopam significantly
800 increased cilia length (**Figure 6C-D**). Notably, CT-Fe₂O₃-NPs also enabled remote
801 manipulation of cilia movement and function *via* an external magnetic field (**Figure 6E**).
802 Cilia function was assessed by monitoring changes in cytosolic Ca²⁺ concentrations.
803 Application of a magnetic field caused significant cilia bending and a sustained rise in Ca²⁺
804 signaling within both the cilioplasm and cytoplasm in cells treated with cilia-targeted
805 nanoplasts, compared to controls (**Figure 6F**). In the *in vivo* study, localization of CT-
806 Fe₂O₃-NPs in the vascular endothelium was confirmed at 24 h and 72 h post-injection. Cilia
807 length was notably increased in mice treated with CT-Fe₂O₃-NPs or CT-M-Fe₂O₃-NPs
808 (under magnetic field exposure) but not in those receiving a 30-min fenoldopam infusion
809 (**Figure 6G**). The results in this section demonstrated that controlling ciliary movement to
810 block the conduction of mechanical signals can achieve efficient tumor treatment.

811 **5.2 Interfering protein biomechanical sensing-transduction function**

812 The oncogenic activity of YAP is controlled by the Hippo kinase cascade and
813 mechanical-force-induced actin remodeling. Li *et al.* from Okinawa Institute of Science and

814 Technology Graduate University developed molecular self-assembly technology to
815 selectively inhibit cancer cell proliferation by inactivating YAP (**Figure 7A**) [193]. In this
816 study, a ruthenium-complex-peptide precursor molecule was engineered to self-assemble
817 into nanostructures under alkaline phosphatase action (**Figure 7B**). These nanostructures
818 were designed to stabilize the lipid rafts of ovarian cancer cells. Upon stabilization, they
819 trigger actin cytoskeleton remodeling (**Figure 7C**), with a particular focus on disrupting F-
820 actin. This actin reorganization subsequently activates LATS, promoting YAP
821 phosphorylation through Hippo signaling. To confirm YAP inactivation, time-lapse
822 immunofluorescence staining of YAP in SKOV3 cells was conducted following 3a
823 incubation, revealing clear inhibition of YAP nuclear translocation after 12 h (**Figure 7D**).
824 Enhanced YAP phosphorylation deactivates YAP, suppressing TEAD-mediated target
825 genes such as connective tissue growth factor (CTGF) and CYR61 (**Figure 7E**), ultimately
826 inhibiting cancer cell proliferation *in vitro* and reducing ovarian tumor growth *in vivo*.

827 Molecular self-assembly technology has demonstrated strong anti-proliferative effects
828 in various cancer cell lines and mouse xenograft models. In SKOV3-Luc xenograft mice,
829 untreated tumors continued to grow throughout the 24-day observation period, while 3a-
830 treated mice showed dose-dependent tumor suppression as early as 4 days post-injection.
831 A 25 mg/kg dose of 3a reduced mean tumor volume by about 60% by day 16 compared to
832 controls. By day 24, tumor volume was reduced by 45% and 60% in groups receiving 25
833 mg/kg and 50 mg/kg doses, respectively (**Figure 7F-G**). In summary, this strategy, which
834 inhibits tumor growth by modulating YAP activity, offers a promising biomechanical
835 regulatory approach to tumor nanotherapeutic strategy.

836 **5.3 Interfering cytoskeletal biomechanical sensing-transduction function**

837 **5.3.1 Electrostimulation disrupts cytoskeletal structure and function**

838 Based on the literature, it has been observed that tumor cells exhibit a comparatively
839 higher susceptibility to external stimulation than normal cells, particularly with regards to
840 their cytoskeletal structure [197]. For instance, Jin's group from State Key Laboratory of
841 Electroanalytical Chemistry of Chinese Academy of Sciences [198] demonstrated that
842 electrostimulation (ES) significantly inhibits glucose and energy metabolism in cancer cells,
843 resulting in rapid cell death (**Figure 8A-C**). From a mechanical perspective, ES leads to
844 cytoskeletal disruption (**Figure 8D**), which reduces the Young's modulus of MCF-7 cell

845 membranes (**Figure 8E**) due to the depolymerization of F-actin and the down regulation
846 and irregular distribution of glucose transporter 1 (GLUT1) (**Figure 8F**). This effect
847 highlights the potential of ES as a highly effective approach for clinical cancer treatments.
848 Experiments reveal that high frequencies and cyclic pressures are primarily responsible
849 for the disruption of actin fibers. Particularly, higher frequency and negative pressures in
850 the latter half of the cycle induce greater tensile strain and deformation, leading to the
851 breakdown of F-actin fibers and increased fluidization.

852 **5.3.2 Low-intensity ultrasound disrupts cytoskeletal structure and function**

853 As for another external stimulation, low-intensity ultrasound (LIUS) is widely used in
854 medicine due to its non-invasive nature, safety, and ability to precisely target and
855 manipulate biological tissues. The ultrasonic cavitation effect of LIUS involves the dynamic
856 expansion and collapse of submicron air pockets, also known as cavitation nuclei, within a
857 fluid when the sound pressure surpasses a certain threshold [199]. The impact of LIUS on
858 the cytoskeleton is pronounced, especially in tumor cells. Recently, Song *et al.* [200]
859 discovered that Piezo1 plays a role in the apoptosis of pancreatic cancer cells when
860 subjected to ultrasound (US) combined with microbubbles (MBs). However, since MBs
861 used in this study are micron-sized, their ideal application *in vivo* presents certain
862 challenges. Following treatment with US and MBs, tumors displayed slower growth rates;
863 however, the growth rate remained higher in the US + MBs + Lv-siPiezo1 group compared
864 to the US + MBs + Lv-NC group. This research emphasized the potential of using
865 ultrasound alongside microbubbles as a non-invasive approach for treating pancreatic
866 ductal adenocarcinoma through mechanotransduction. Additionally, other studies have
867 shown that this combination can effectively disrupt the cytoskeletal structure of tumor cells
868 by generating intense mechanical forces [201, 202]. However, the micrometer size of MBs
869 may limit their *in vivo* application, and achieving Piezo1 overexpression *in vivo* is
870 challenging due to its high molecular weight. Overcoming these challenges will be crucial
871 for future clinical applications.

872 **5.4 Interfering ECM-cellular membrane biomechanical sensing-transduction** 873 **function**

874 **5.4.1 Interfering the mechanical properties of ECM**

875 The TME exhibits increased stiffness due to an abundance of ECM, which amplifies

876 its intrinsic mechanical properties [203]. These 'inside-out' tensile forces are primarily
877 mediated through integrin-dependent cell adhesions involving FAK activation [204].
878 Consequently, targeting FAK in tumor tissue can modulate the mechanical properties of
879 tumor and stromal cells as well as the tumor ECM. CRISPR/Cas genome editing offers
880 substantial potential for cancer treatment by enabling precise inactivation or repair of
881 cancer-related genes. A study developed multiplexed nanoparticles designed to deliver
882 siFAK to disrupt the ECM, Cas9 mRNA to express Cas protein, and targeted sgRNA to
883 knockout specific cancer genes [205]. FAK inhibition was shown to reduce tumor cell
884 contractility and membrane tension, along with ECM stiffness, thereby enhancing CRISPR
885 gene editing efficiency in tumor cells both *in vitro* and *in vivo* by promoting lipid
886 nanoparticles (LNPs) endocytosis and tumor penetration. *In vivo* results further
887 demonstrated that siFAK + CRISPR-LNPs decreased metastatic potential in an ovarian
888 cancer mouse model, improved outcomes in a tumor xenograft mouse model, and
889 extended survival in an aggressive MYC-driven liver cancer model, highlighting significant
890 anti-tumor effects across different cancer types.

891 **5.4.2 Disrupting cellular membrane integrity**

892 The cellular membrane, composed of a lipid bilayer and cell surface receptors, detects
893 mechanical signals from the environment and transmits this information to the intracellular
894 cytoskeletal machinery. Thus, membrane-disruptive macromolecules can weaken
895 membrane integrity, interfere with biomechanical signaling, and reduce the ability of cells
896 to adhere to the stroma or neighboring cells. Yang's group from University of Science and
897 Technology of China [206] demonstrated the feasibility of acid-responsive nanoparticles
898 composed solely of membrane-disruptive molecules for treating pancreatic cancer with
899 dense stromal barriers (**Figure 9A**). Using a pH-sensitive micelle derived from a polymeric
900 mimic of host defense peptides as the core of the nanoplatform, the acid-activatable
901 nanoparticle (M-14K) showed selective cytotoxicity toward BxPC-3 pancreatic cancer and
902 NIH-3T3 fibroblast cells under mildly acidic conditions (**Figure 9B-C**). These nanoparticles
903 dissociate at the weakly acidic pH of the TME (pH 6.5–6.8) but remain stable at
904 physiological pH (7.4). In a BxPC-3@NIH-3T3 spheroid model, M-14K effectively
905 penetrated the fibroblast layer to target cancer cells at pH 6.8 over 24 h (**Figure 9D**).
906 Intravenous administration in mouse models with BxPC-3 xenograft tumors showed higher

907 uptake of M-14K compared to its pH-insensitive counterpart (M-35K) (**Figure 9E**), with
908 delivery efficiency 12.3 times that of M-35K (0.74% vs. 0.06%) (**Figure 9F**). Throughout
909 the observation period, M-14K treatment significantly delayed tumor growth (**Figure 9G**)
910 without causing off-target effects. Overall, this strategy provides a promising translational
911 approach for improving pancreatic cancer treatment by disrupting cellular membrane
912 integrity, permeating the stromal barrier, and interfering with biomechanical signaling.
913 Although these pH-sensitive nanoplateforms show promise in treating pancreatic cancer,
914 their non-biodegradability, limited cell selectivity, and model limitations remain significant
915 drawbacks that must be addressed in future research.

916 **5.5 Interfering TME-biomechanical sensing-transduction function**

917 In photodynamic therapy (PDT), the solid stress in stroma-rich tumors can hinder
918 photosensitizer delivery. To address this, Chen *et al.* from Huazhong University of Science
919 and Technology [207] proposed a strategy to enhance PDT efficacy by combining
920 hydroxyethyl starch–chlorin e6 conjugate nanoparticles (HES–Ce6 NPs) with the TGF- β
921 inhibitor LY2157299 (LY) (**Figure 10A**). Prior to PDT, LY administered intragastrically
922 downregulated TGF- β signaling and ECM-related mRNA expression (**Figure 10B**),
923 reduced collagen deposition (**Figure 10C**), alleviated solid stress (**Figure 10D**), and
924 decompressed tumor blood vessels. This pretreatment significantly promoted HES–Ce6
925 NP penetration in tumors (**Figure 10E**), allowing the restructured tumor microenvironment
926 to improve the accumulation and penetration of HES–Ce6 NPs, ultimately enhancing the
927 anti-tumor efficacy of PDT (**Figure 10F**).

928 In a separate study, Cong *et al.* from Yanshan University [208] developed a “nano-
929 lymphatic” system (DOX/g-C₃N₄/luminol@cytomembrane, DCL@M) aimed at addressing
930 the elevated tumor IFP resulting from lymphatic insufficiency. In this system, lactic acid
931 serves as a sacrificial agent, while DCL@M facilitates photocatalytic water splitting to
932 reduce the volume of interstitial fluid, thereby mitigating the resistance to transfer caused
933 by high tumor interstitial fluid pressure. The *in vivo* experiments demonstrated a significant
934 62.11% reduction in tumor IFP within the tumor tissue, which subsequently improved blood
935 perfusion. The accumulation of the “nano-lymphatic” system (16.73%) in the tumor was
936 found to be 15.9 times and 3.31 times greater than that of free doxorubicin hydrochloride
937 (DOX, 1.05%) and DOX/g- C₃N₄@cytomembrane (DC@M, 3.03%), respectively. This

938 indicates that the “nano-lymphatic” approach offers a novel strategy for enabling
939 nanodrugs to navigate biological barriers and enhance therapeutic efficacy. Overall, these
940 innovative strategies hold promise for advancing cancer treatments by overcoming the
941 physical and mechanical challenges present within the tumor microenvironment. Although
942 this research has highlighted the significant potential of the 'nano-lymphatic' system in
943 tumor treatment, its clinical translation remains challenging. Issues such as biological
944 safety, large-scale production difficulties, and individual patient variability can impact the
945 efficacy of the 'nano-lymphatic' system, necessitating the integration of personalized
946 treatment plans and precision medicine.

947 **6. Conclusions, challenges and prospectives**

948 Tumors and tumor microenvironments complement each other, jointly promoting the
949 growth, invasion, metastasis, and drug resistance of tumor cells. Therefore, effective tumor
950 treatment strategies should regulate the tumor microenvironment simultaneously.
951 Compared with chemical drugs, macromolecular drugs, and cell therapy, the main
952 advantage of biomechanical based cancer treatment strategies is that: i) biomechanics can
953 macroscopically regulate the function of cell secondary structures, such as primary cilia,
954 cytoskeleton, etc., rather than targeting a single target or a specific type of cell. Therefore,
955 the scope of regulation based on biomechanics is broad and has multiple impacts on tumor
956 progression. For example, the regulation of the cytoskeleton can simultaneously affect
957 DNA damage repair, metastasis, and drug resistance in tumor cells. This widespread effect
958 makes the tumor suppressive effect stronger and less likely to develop tolerance. ii) The
959 biomechanical regulation methods have the characteristic of diversity, which can be small
960 molecule drugs or mechanical effects applied *in vitro*, such as low-intensity focused
961 ultrasound, ultrasound cavitation, etc. Regulating tumor cells through physical means
962 rather than chemically active biomolecules can significantly reduce common toxic side
963 effects in tumor treatment, such as nausea, immune system suppression, and organ
964 damage. However, the investigation of how biomechanics affect the onset and progression
965 of cancer remains relatively underexplored. Mechanical imbalance is a significant feature
966 of malignant tumor tissues, suggesting that disruptions in mechanical homeostasis may
967 precede tumorigenesis and tumor advancement. A deeper exploration of biomechanics
968 could facilitate earlier and more precise detection of cancer development and tumor

969 formation, while also expanding the conversation about the various factors that contribute
970 to cancer progression. This review presents a thorough overview of the known mechanical
971 properties linked to malignant tumors. By synthesizing the molecular and mechanical
972 characteristics at both cellular and tissue levels across different cancers, researchers can
973 better focus on applying mechanobiology to the study of malignant conditions.

974 This paper analyzed the impact of the tumor mechanical environment on the
975 occurrence and development of tumor angiogenesis, tumor drug resistance, and tumor
976 metastasis. Mechanoreceptors initially detect mechanical signals from the TME and
977 subsequently interact with mechanosignaling proteins to transduce these mechanical
978 signals into biological signals, thereby modulating cellular responses, gene expression,
979 and tumor microenvironment. The multidimensional mechanical forces experienced by
980 tumors create abnormal tumor vasculature and morphological structures, leading to
981 specific therapies such as nanodrug-mediated embolization treatment and tumor
982 vasculature normalization induction strategies. All proteins acting as mechanosensors and
983 the involved signaling networks have provided new therapeutic targets and challenges in
984 overcoming tumor metastasis and drug resistance mechanisms.

985 Innovative bioengineering technologies and novel therapeutic strategies for
986 biomechanical regulation offer transformative potential in tumor therapy by addressing the
987 mechanical properties of cancer cells and their microenvironment. These technologies,
988 such as targeted drug delivery systems and molecular self-assembly, enable precise
989 control over cellular biomechanics, crucial for effective treatment. For instance, primary
990 cilia-targeted nanoparticles enhance drug delivery and therapeutic efficacy by specifically
991 targeting and modulating cilia functions. Additionally, advancements in
992 mechanotransduction, such as using small molecules to inhibit key signaling pathways or
993 employing low-intensity ultrasound to disrupt cytoskeletal structures, demonstrate
994 significant promise in altering tumor progression and enhancing treatment outcomes. The
995 integration of nanotechnology into biomechanical regulation strategies holds immense
996 potential for revolutionizing cancer treatment. Ultimately, expanding research into
997 mechanical properties and their impact on tumor behavior will enhance our understanding
998 of cancer and lead to more effective, personalized therapies.

999 Nevertheless, the main challenge of biomechanical tumor treatment strategies lies in

1000 the translation of mechanobiological principles into clinical practice. Firstly, current
1001 research lacks simplifying and standardizing methods for measuring mechanical properties.
1002 The complexity of current technologies requires advancements to make them more
1003 accessible for clinical use. Secondly, while analyzing the adaptation of tumors to the
1004 surrounding mechanical environment, we also realize the significant gaps remain in our
1005 understanding of the complex interactions between mechanoreceptors, mechanosensors,
1006 and tumor progression. Current experimental models often fail to capture the dynamic
1007 mechanical interactions within tumors, highlighting the need for more sophisticated models.
1008 Thirdly, current research focuses on the therapeutic effect on tumors, while ignoring the
1009 safety of strategies based on mechanical signal interference. Subsequent research must
1010 further enhance the tumor targeting of therapeutic agents to reduce crosstalk with
1011 biomechanical signals of normal tissues. Finally, the therapeutic effects of combined
1012 treatment approaches based on tumor biomechanical regulation remain to be developed.
1013 For instance, prior to chemotherapy, physical methods like low-intensity ultrasound or
1014 electrical stimulation can be employed to disrupt the cytoskeletal structure of tumor cells,
1015 thereby reducing their drug resistance and enhancing the permeability and efficacy of
1016 chemotherapeutic agents. Similarly, inhibiting integrin-mediated cell-matrix adhesion
1017 signaling can decrease the adhesion force between tumor cells and the ECM, diminishing
1018 their ability to colonize other tissues. With the increasing attention and the continuous
1019 breakthrough of technical barriers, more patients will benefit from biomechanical regulation
1020 tumor therapeutic strategies.

1021

1022 **Abbreviations**

1023 ECM, extracellular matrix; MS, mechanosensitive; AFM, atomic force microscopy; MPA,
1024 micropipette aspiration; TFM, traction force microscopy; TME, tumor microenvironment;
1025 MMPs, matrix metalloproteinases; HA, hyaluronic acid; IFP, interstitial fluid pressure; CAFs,
1026 cancer-associated fibroblasts; TAMs, tumor-associated macrophages; ECs, endothelial
1027 cells; HCC, hepatocellular carcinoma; PDAC, pancreatic ductal adenocarcinoma; MVP,
1028 microvascular pressure; GPCRs, G protein-coupled receptors; CTCs, circulating tumor
1029 cells; MTs, microtubules; ABC, ATP-binding cassette; YAP, yes-associated protein; TAZ,
1030 transcriptional coactivator with PDZ-binding motif; GCX, glycocalyx; GAG,

1031 glycosaminoglycan; HS, heparan sulfate; PC, primary cilia; PDAC, pancreatic ductal
1032 adenocarcinoma; PitNETs, pituitary neuroendocrine tumors; RAR, retinoic acid receptor;
1033 CREB, cAMP-response element binding protein; ATP, adenosine triphosphate; TRP,
1034 transient receptor potential; TRPM7, transient receptor potential melastatin 7; FAK, focal
1035 adhesion kinase; EMT, epithelial-mesenchymal transition; EGFR, epidermal growth factor
1036 receptor; CXCR4, C-X-C chemokine receptor type 4; CCR5, C-C chemokine receptor 5;
1037 GDP, guanosine diphosphate; GTP, guanosine triphosphate; ROCK, rho-associated
1038 coiled-coil-containing protein kinase; PAKs, p21-activated kinases; EPR, enhanced
1039 permeability and retention; LPAR1, lysophosphatidic acid receptor 1; LPA,
1040 lysophosphatidic acid; CT, cilia-targeted; GCX, glycocalyx; GAG, glycosaminoglycan;
1041 CTGF, connective tissue growth factor; ES, electrostimulation; GLUT1, glucose transporter
1042 1; LIUS, low-intensity ultrasound; US, ultrasound; MBs, microbubbles; LNPs, lipid
1043 nanoparticles; M-14K, acid-activatable nanoparticle; PDT, photodynamic therapy; HES–
1044 Ce6 NPs, hydroxyethyl starch–chlorin e6 conjugate nanoparticles; LY, TGF- β inhibitor
1045 LY2157299; DCL@M, DOX/g-C₃N₄/luminol@cytomembrane; DOX, doxorubicin
1046 hydrochloride; DC@M, DOX/g-C₃N₄@cytomembrane; TGF- β , transforming growth factor-
1047 β ; DP, guanosine diphosphate; GLUT1, glucose transporter 1; GO, graphene oxide.

1048

1049 **Acknowledgements**

1050 This study was financially supported by the National Natural Science Foundation of China
1051 (Grant No. 82103505, 82273348, 82473165, 82171939, W2421099, and 82471986), the
1052 Science and Technology Program of Zhejiang Province (Grant No. 2024C03159), the
1053 National Key R&D Program of China (Grant No. 2022YFC2704200, 2022YFC2704203,
1054 and 2021YFC2701204), and the Natural Science Foundation of Zhejiang Province (Grant
1055 No. ZCLY24H1602 and LQ23H180006).

1056

1057 **Competing Interests**

1058 The authors have declared that no competing interest exists.

1059

1060 **Author contributions**

1061 **Xiaodong Wu:** Data curation, Visualization, Writing – original draft, Writing – review &
1062 editing, Funding acquisition. **Weidong Fei:** Software, Data curation, Writing – original draft,
1063 Writing – review & editing, Funding acquisition. **Tao Shen:** Resources, Writing – review &
1064 editing. **Lei Ye:** Resources, Writing – review & editing. **Chaoqun Li:** Data curation, Writing
1065 – review & editing. Siran Chu: Data curation, Writing – review & editing. **Mingqi Liu:** Data
1066 curation, Writing – review & editing. **Xiaodong Cheng:** Supervision, Project administration,
1067 Funding acquisition. **Jiale Qin:** Software, Supervision, Data curation, Funding acquisition,
1068 Writing – review & editing.

1069

1070

1071

1072

1073

1074

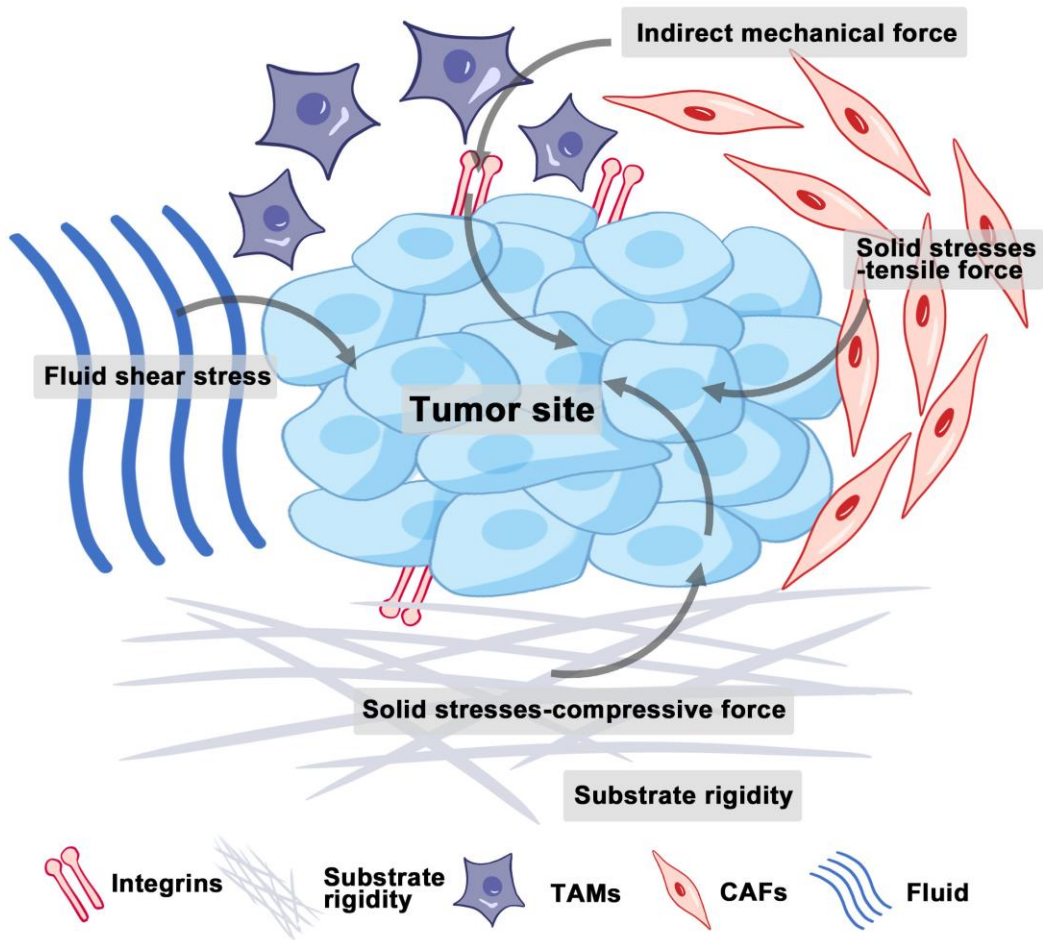
1075

1076

1077

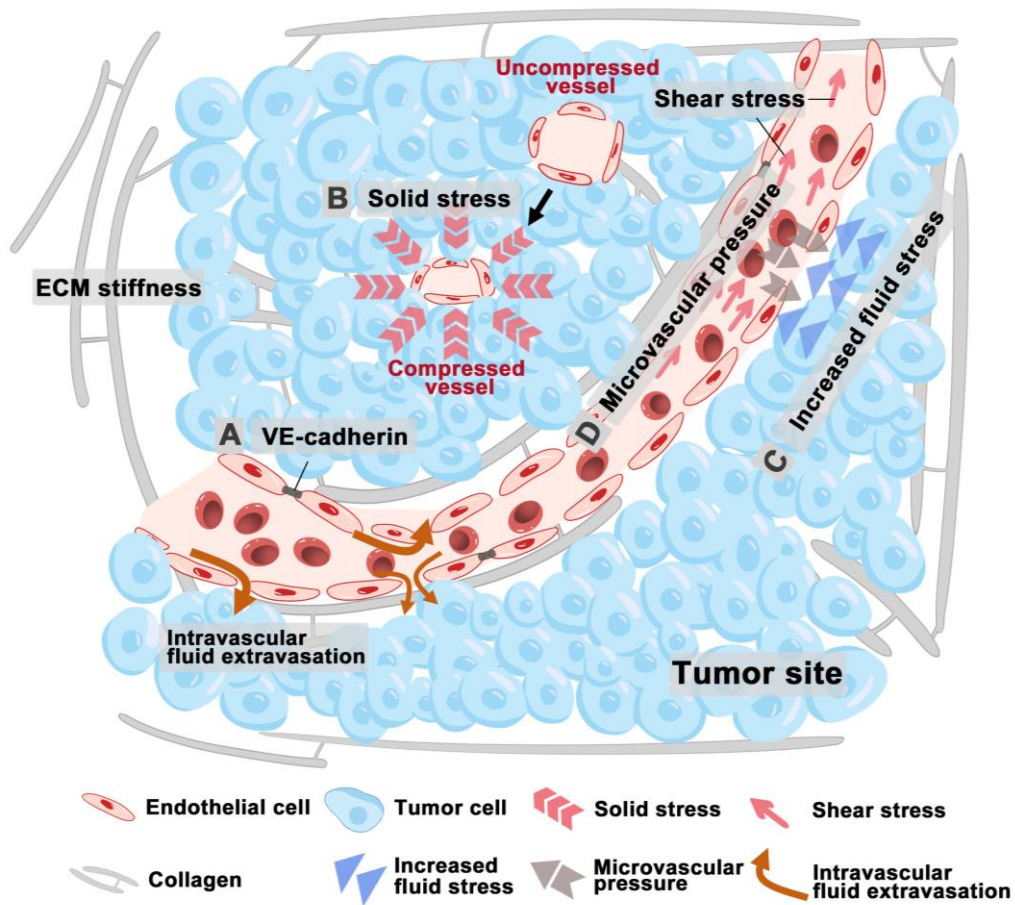
1078

1079



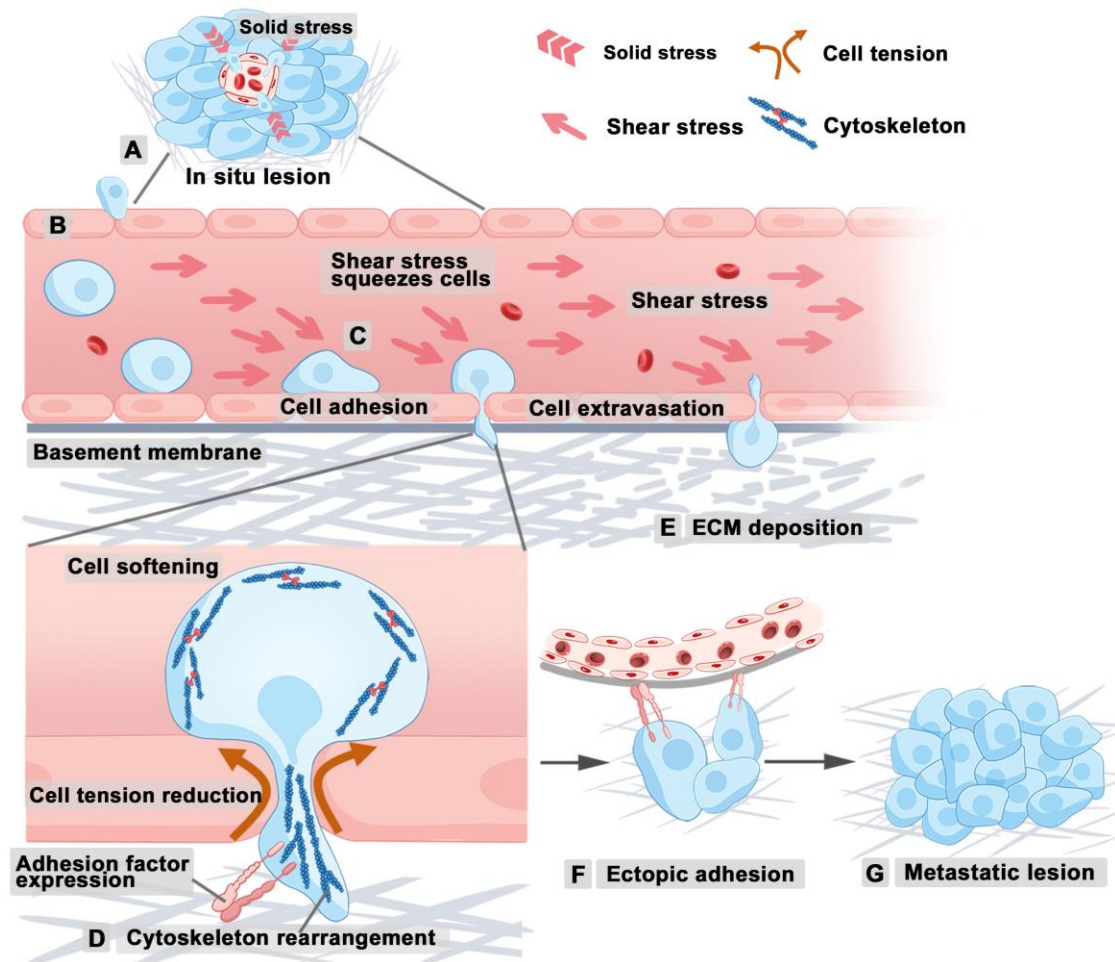
1081 **Figure 1.** Mechanical forces at the tumor site. Solid stresses encompass both tensile and
 1082 compressive forces. Increased fluid and hydrostatic pressure result from fluid extravasation
 1083 from blood vessels and secretions from stromal cells. Indirect mechanical forces are
 1084 relayed by CAFs and TAMs to mechanosensors. Abbreviations: CAFs, cancer-associated
 1085 fibroblasts; TAMs, tumor-associated macrophages. (Adapted with permission from Ref.
 1086 [163]. Copyright 2020 Ivyspring International Publisher)

1087
 1088
 1089
 1090
 1091
 1092
 1093



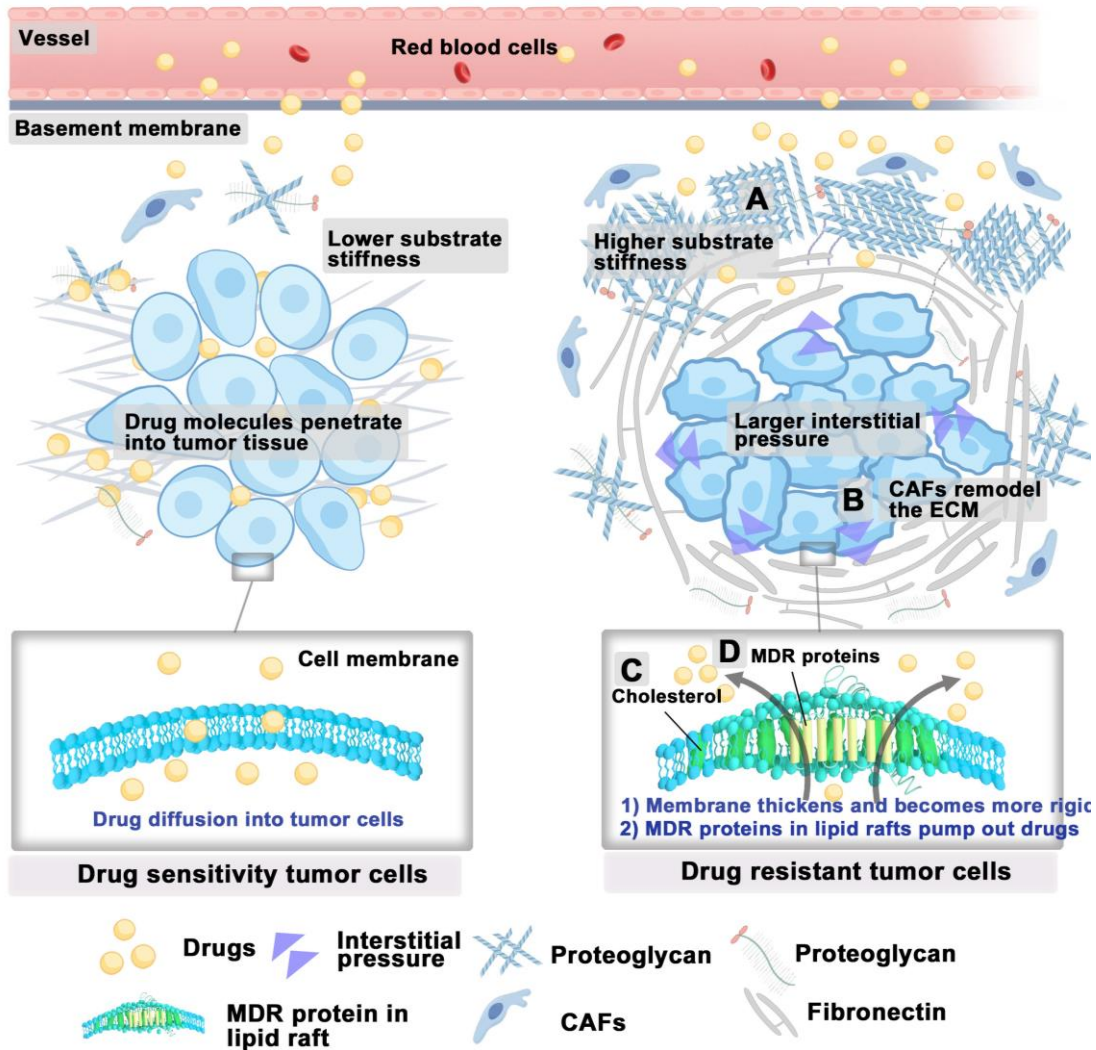
1094 **Figure 2.** Mechanical forces within the tumor microenvironment impact tumor
 1095 angiogenesis. (A) ECM stiffening alters cell-cell junctions and the positioning of VE-
 1096 cadherin, thus disrupting barrier integrity and increasing permeability. (B) Solid stress
 1097 compresses tumor vessels. (C) Increased fluid stress results in abnormal vascular
 1098 development and inadequate tissue perfusion. (D) Elevated IFP within tumors often
 1099 surpasses MVP, thereby limiting perfusion and disturbing flow patterns. Abbreviations:
 1100 ECM, extracellular matrix; IFP, interstitial fluid pressure; MVP, microvascular pressure.

1101
 1102
 1103
 1104
 1105
 1106



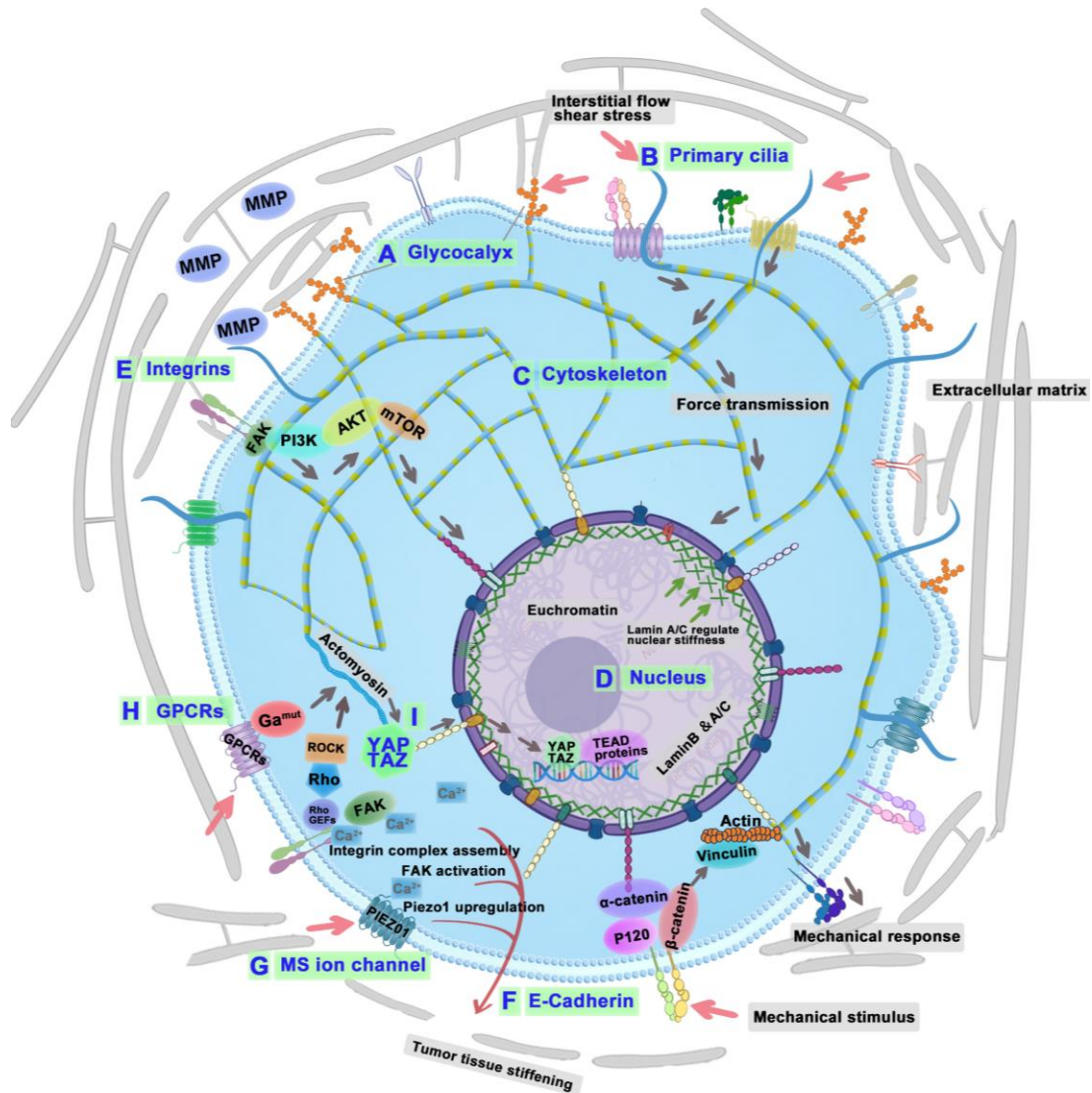
1107 **Figure 3.** Tumor cell metastasis under biomechanical influence. (A) Tumor cells lose
 1108 adhesion and detach from tumor tissue. (B) Tumor cells disrupt endothelial junctions,
 1109 enabling entry into blood vessels. (C) Hydrodynamic shear stress converts CTCs into
 1110 flexible cancer stem cells, enhancing their mimicry of ECs and promoting metastasis. (D)
 1111 The cytoskeleton regulates tumor cell stiffness and penetration. (E) MMPs degrade the
 1112 ECM, facilitating tumor cell passage through the vascular basement membrane. (F) Tumor
 1113 cells adhere to blood or lymphatic vessels. (G) Metastatic tumor forms. Abbreviations: ECM,
 1114 extracellular matrix; CTCs, circulating tumor cells; ECs, endothelial cells; MMPs, matrix
 1115 metalloproteinases. (Adapted with permission from Ref. [209]. Copyright 2024 Springer
 1116 Nature)

1117
 1118
 1119
 1120



1121 **Figure 4.** The biomechanical environment of drug-resistant tumor cells. (A) High collagen
 1122 deposition in the ECM increases stiffness, contributing to drug resistance. (B) CAFs modify
 1123 the ECM, promoting drug tolerance. (C) Elevated cholesterol levels in cancer cells, leading
 1124 to thicker membranes that reduce drug permeability. (D) Increased cholesterol in lipid rafts
 1125 enhances the function of multidrug resistance transporters, facilitating drug transport and
 1126 contributing to drug resistance. Abbreviations: ECM, extracellular matrix; CAFs, cancer-
 1127 associated fibroblasts.

1128
 1129
 1130
 1131
 1132



1133 **Figure 5.** Diagram of tumor cell biomechanical perception, conduction, and effect
 1134 mechanism. The GCX (A), primary cilium (B), cytoskeleton (C), and nucleus (D) of tumor
 1135 cells sense the surrounding mechanical signals; integrins (E), cadherins (F), MS ion
 1136 channels (G), GPCRs (H), and YAP/TAZ (I) convert physical signals into biological signals.
 1137 Decoding biomechanical signaling mechanisms of cancer cells: GCX senses shear stress
 1138 and helps integrin clustering-MMP expression-tumor metastasis; PC senses fluid flow-
 1139 influence cilia assembly-tumorigenesis and tumor progression; Cytoskeleton senses and
 1140 transduces mechanical stresses-cytoskeletal remodeling-tumor metastasis; Nucleus
 1141 senses mechanical cues-calcium channels regulation-DNA repair-tumor therapy
 1142 resistance; Nucleus regulate lamin A-YAP and RAR-cytoskeleton regulation; Integrins
 1143 interact with ECM components-regulates cytoskeleton-tumor metastasis; Cadherins
 1144 convey mechanical signals-EGFR, catenins, and YAP-tumor proliferation, migration, and

1145 invasion; GPCRs mediate mechanotransduction-YAP signaling pathway-tumor
1146 progression and metastasis; MS ion channels convert biochemical signals-Piezo1 initiate
1147 integrin-FAK signaling-tumor invasion; TRPM7-activate EMT pathway-tumor metastasis;
1148 YAP/TAZ convert mechanical signal-matrix stiffness-tumor invasion.

1149 Abbreviations: GCX, glycocalyx; PC, primary cilia; YAP, yes-associated protein; RAR,
1150 retinoic acid receptor; ECM, extracellular matrix; EGFR, epidermal growth factor receptor;
1151 GPCRs, G protein-coupled receptors; EMT, epithelial-mesenchymal transition; MS,
1152 Mechanosensitive; TRPM7, transient receptor potential melastatin 7; YAP/TAZ, yes-
1153 associated protein/transcriptional coactivator with PDZ-binding motif.

1154

1155

1156

1157

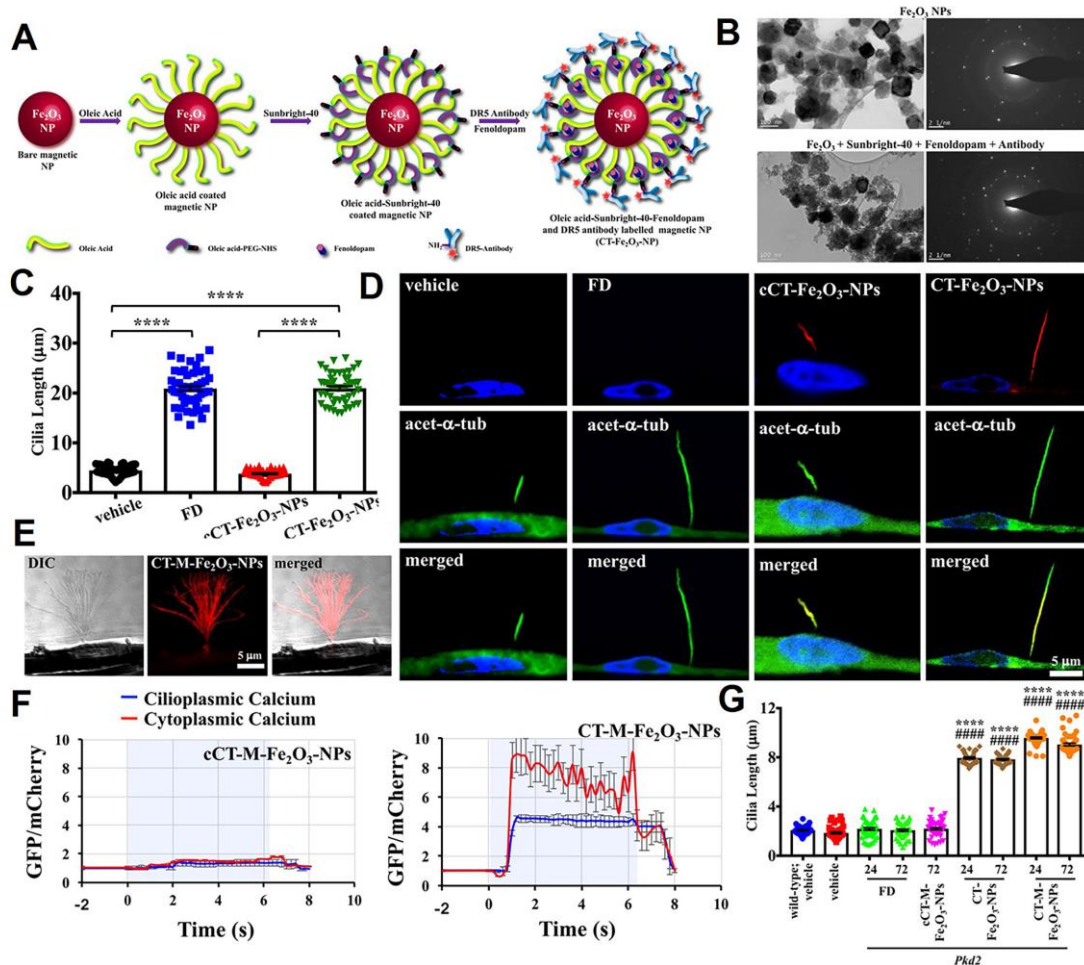
1158

1159

1160

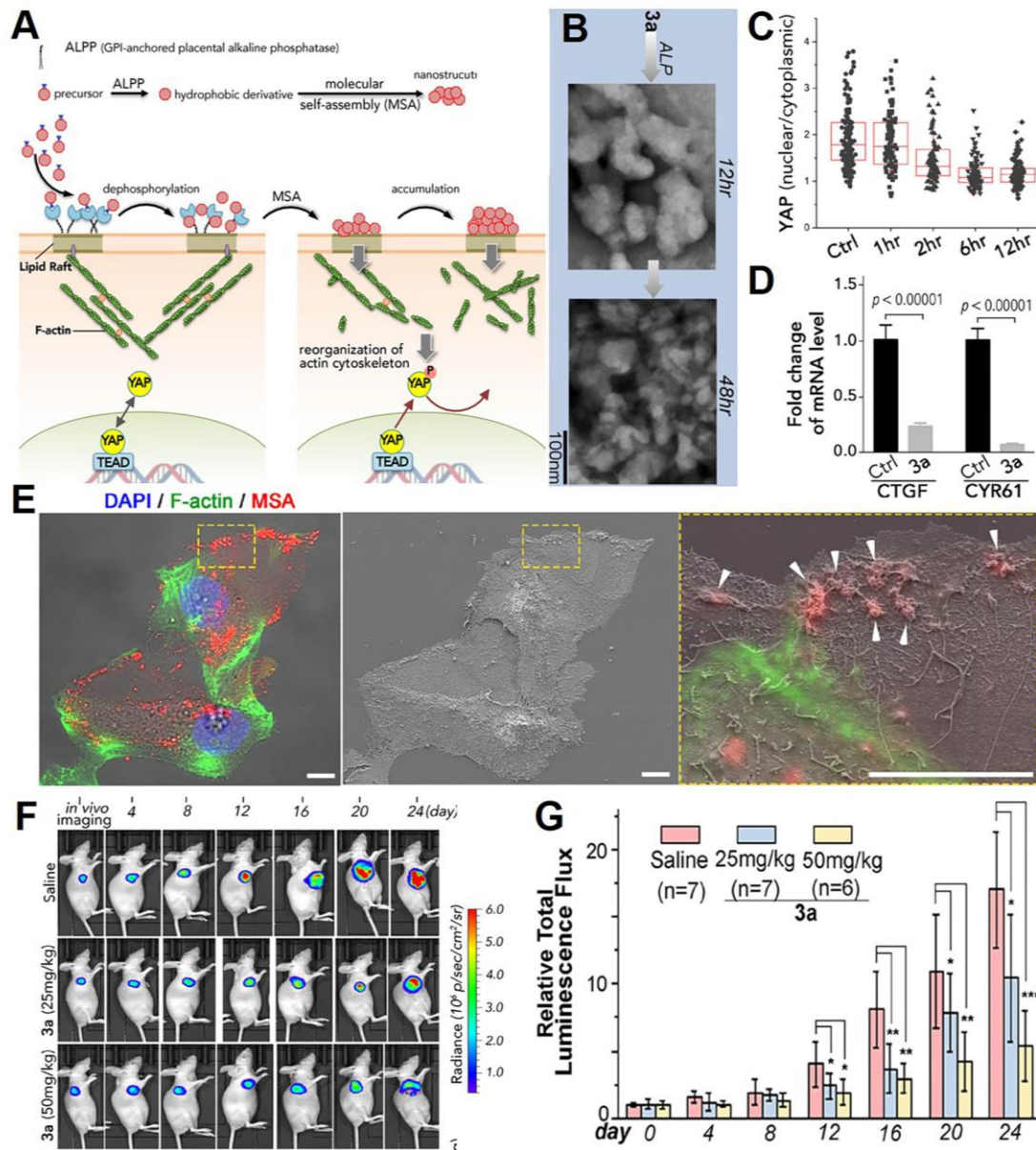
1161

1162

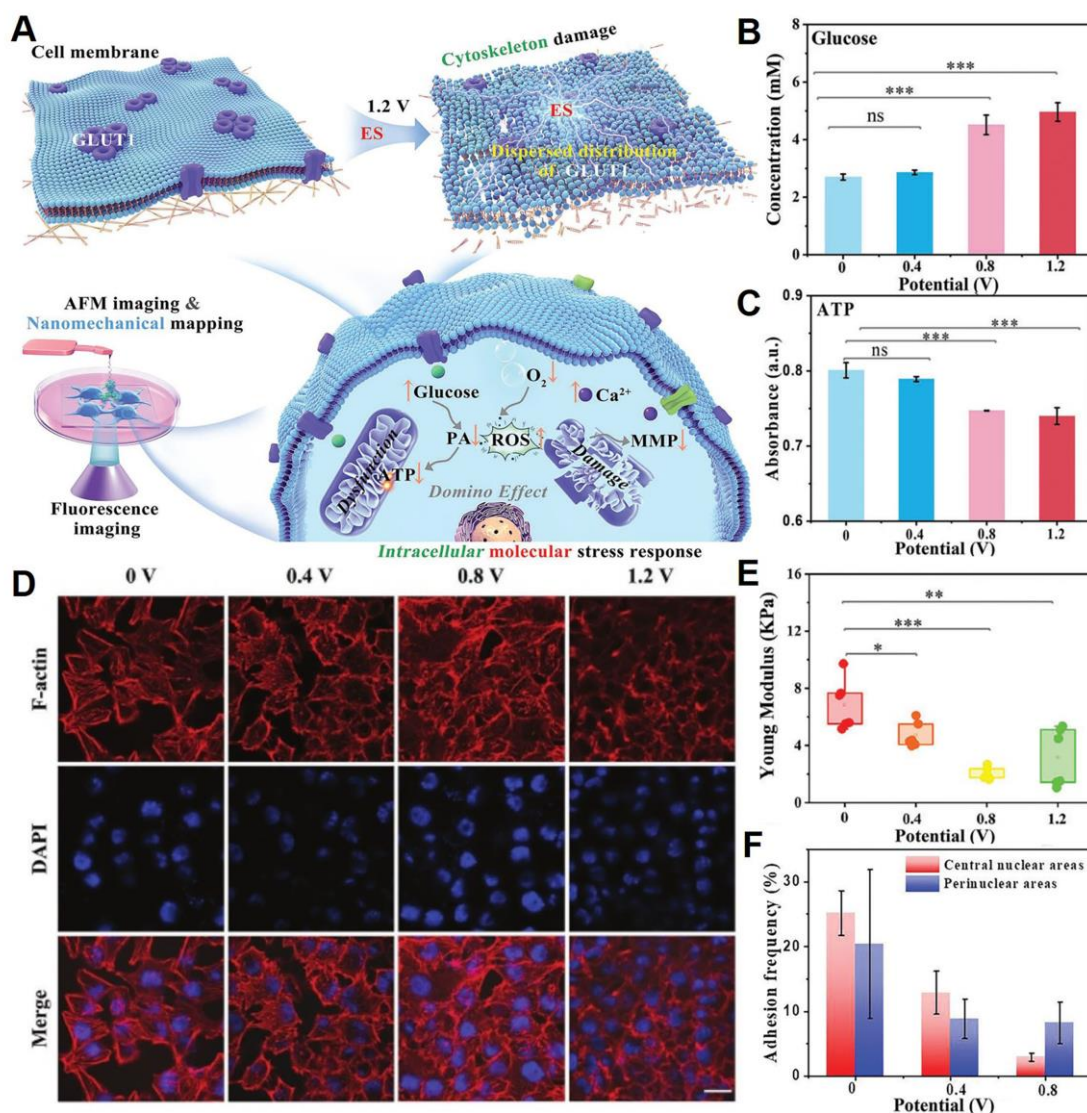


1163 **Figure 6.** Design nanoplatforms for interfering with the biomechanical function of primary
 1164 cilia. (A) Synthesis and surface functionalization of CT- Fe_2O_3 -NPs. (B) TEM and selected
 1165 area electron diffraction images of bare Fe_2O_3 -NPs and CT-M- Fe_2O_3 -NPs. (C) A
 1166 representative dot-plotted bar graph displaying the ciliary lengths measured in cells
 1167 subjected to various treatments. (D) Fluorescence images illustrating that both fenoldopam
 1168 and CT- Fe_2O_3 -NPs (red) resulted in increased cilia length. (E) An external magnetic field
 1169 applied to CT-M- Fe_2O_3 -NPs induced passive movements of the cilia. (F) Line graphs
 1170 depicting average cytosolic (red) and cilioplasmic (blue) Ca^{2+} levels (in arbitrary units). (G)
 1171 Dot-plotted bar graphs showing cilia lengths in vascular endothelial cells. (Adapted with
 1172 permission from Ref. [196]. Copyright 2019 American Chemical Society)

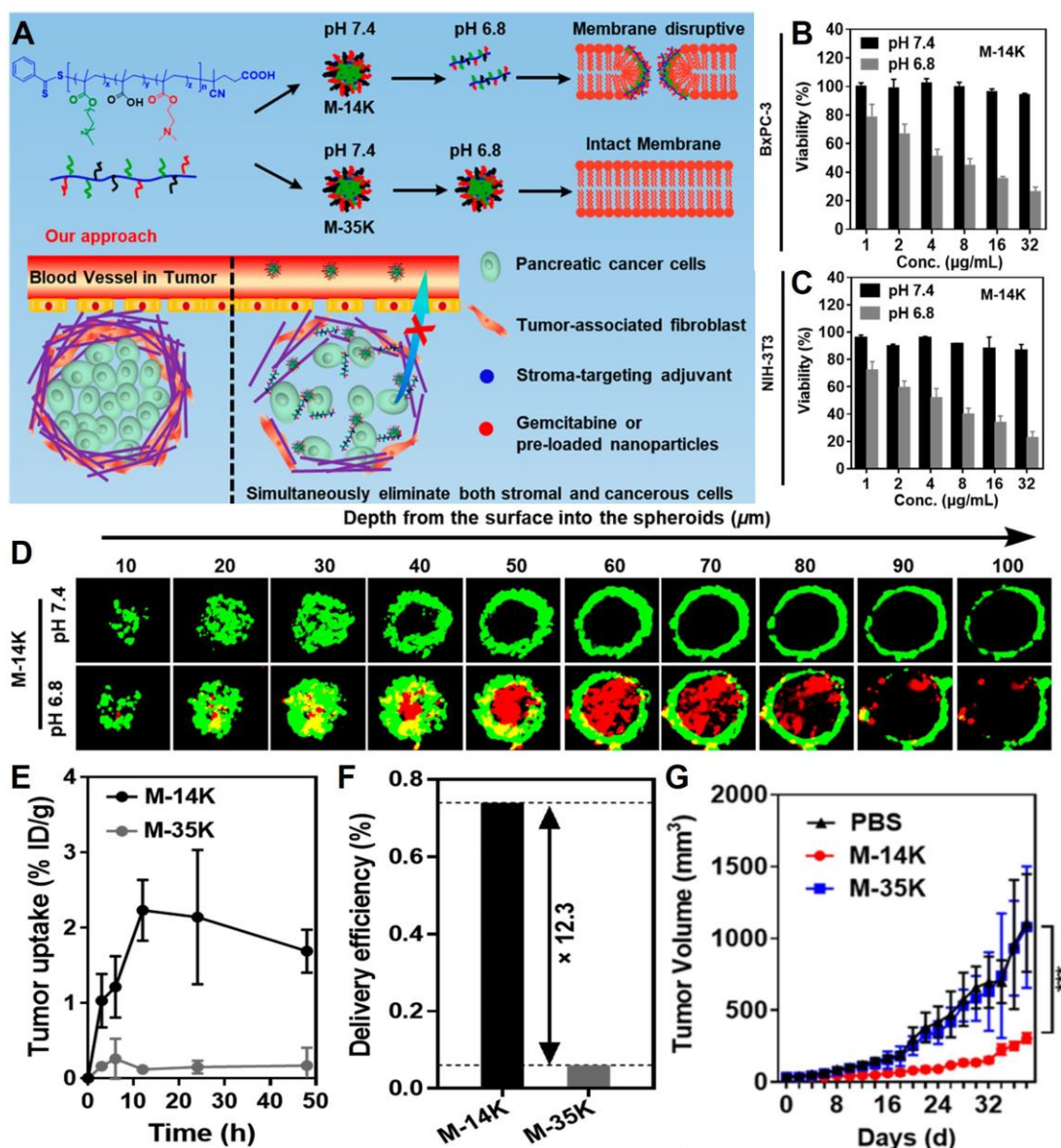
1173
 1174
 1175
 1176



1177 **Figure 7.** Design nanotherapeutics for interfering with the biomechanical transduction
 1178 function of YAP. (A) Schematic illustrating the mechanisms of lipid-raft-targeted
 1179 nanoplatforms for disturbing the YAP through actin cytoskeleton disruption. (B) Alkaline
 1180 phosphatase dephosphorylation of 3a initiates molecular self-assembly at varying time
 1181 points, forming diverse nanostructures. (C) Quantification of YAP intensity ratio between
 1182 the nucleus and cytoplasm in SKOV3 cells at 60-70% confluence after incubation with 3a
 1183 over different time periods. (D) The qPCR analysis of YAP target genes CTGF and CYR61
 1184 in untreated and 3a-treated SKOV3 cells. (E) Correlative light-electron microscopy of HeLa
 1185 cells following incubation with 3a. Tumor growth was monitored (F) and analyzed (G) using
 1186 bioluminescence detection. (Adapted with permission from Ref. [193]. Copyright 2021

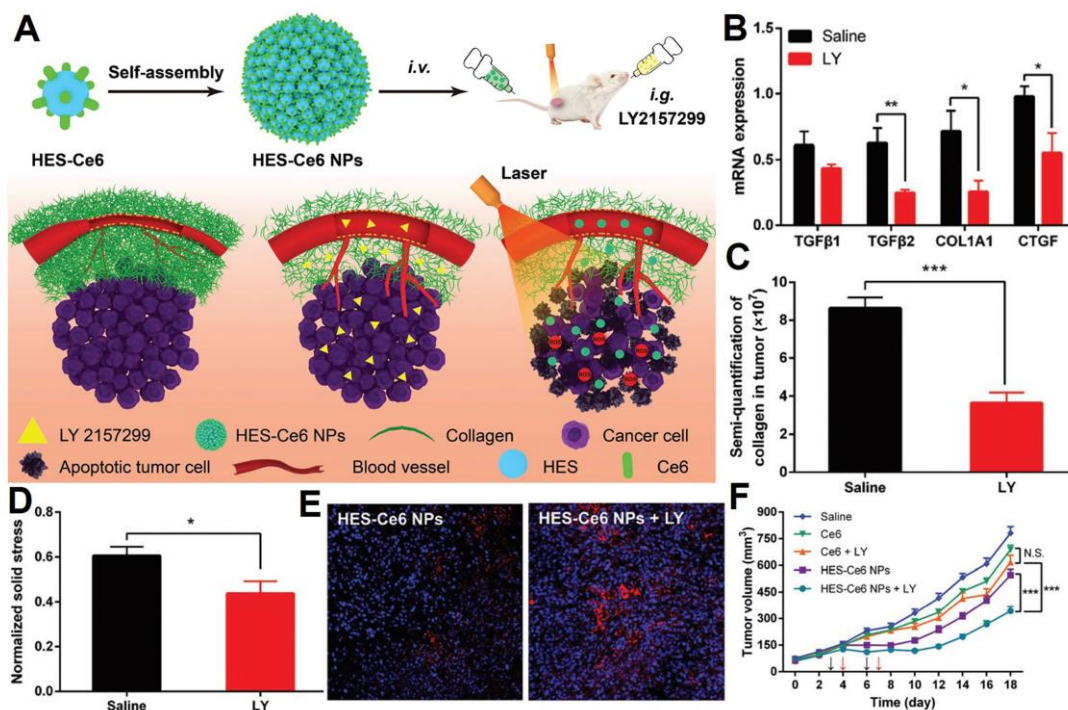


1188 **Figure 8.** Electrostimulation disrupts the structure and function of the cytoskeleton. (A)
 1189 Schematic representation of the molecular and nanomechanical insights into how ES
 1190 inhibits energy metabolism and causes cytoskeletal damage in cancer cells. (B) Glucose
 1191 concentration within MCF-7 cells measured using under different voltage conditions for 5
 1192 min. (C) ATP content in MCF-7 cells treated for 5 min at varying voltages. (D) Fluorescence
 1193 imaging of MCF-7 cells subjected to different voltages for 5 min, showing F-actin (Cy3, red)
 1194 and cell nuclei (DAPI, blue). (E) Statistical analysis of perinuclear Young's modulus (fitted
 1195 using the Cone Sphere model) from MCF-7 cells exposed to different voltages for 5 min.
 1196 (F) Probability statistics of GLUT1 recognition in the nuclear and perinuclear regions of
 1197 MCF-7 cells after ES treatment at different voltages for 5 min. (Adapted with permission
 1198 from Ref. [198]. Copyright 2023 Wiley-VCH)



1199 **Figure 9.** Design nanotherapeutics for disrupting the integrity of the cellular membrane. (A)
 1200 Schematic of acid-activatable, membrane-disruptive nanomicelles (M-14K) designed to
 1201 target both cancer and stromal cells. (B-C) Viability assays for BxPC-3 cancer cells and
 1202 activated NIH-3T3 fibroblasts. (D) Images of three-dimensional BxPC-3@NIH-3T3
 1203 spheroids, showing a fibroblast shell (green) surrounding a core of cancer cells post-M-
 1204 14K treatment; propidium iodide (red) stains the dead cells. (E) Tumor uptake of DiD-
 1205 labeled M-14K and M-35K, and (F) comparison of calculated tumor-targeting efficiency
 1206 between M-14K and M-35K in BxPC-3 tumor-bearing mouse models. (G) Tumor volume
 1207 measurements during treatment. (Adapted with permission from Ref. [206]. Copyright 2021
 1208 American Chemical Society)

1209



1210 **Figure 10.** Design nanoplatforms for interfering with the biomechanical transduction
 1211 function of the tumor microenvironment. (A) Schematic of HES–Ce6 NPs combined with
 1212 TGFβ inhibitors to enhance PDT. (B) The mRNA expression levels of TGF-β1, TGF-β2,
 1213 COL1A1, and CTGF in tumor tissues. (C) Semi-quantitative analysis of collagen in tumors
 1214 using Masson staining. (D) Normalized solid stress measured as the ratio of tumor opening
 1215 to tumor height. (E) Representative images of drug penetration in tumors (blue: DAPI, red:
 1216 Ce6). (F) Tumor growth in 4T1 tumor-bearing mice. (Adapted with permission from Ref.
 1217 [207]. Copyright 2021 Royal Society of Chemistry)

1218
 1219
 1220

Table 1. Clinically used drug on mechanical forces of tumor treatment.

Drugs	Signaling pathway	Functional mechanism	Ref
PEGPH20	HA-tumor solid stress	Degrade HA and decrease solid stresses, enhance perfusion and drug delivery in pancreatic ductile adenocarcinomas	[210]
4-MU	HA-tumor solid stress	Inhibits HA synthesis by down-regulating HA receptors and the phosphatidylinositol 3-kinase/CD44 complex	[88]
A6	A6-CD44-HA	CD44 is a receptor for HA while A6 binds to CD44, resulting in the inhibition of the modulation of CD44-mediated cell signaling including HA	[89]
Bevacizumab	VEGFA-tumor angiogenesis	Prevents VEGFA from binding to receptors, hinders neovascularization and the activation of signal transduction cascades	[32]
Anlotinib	Tyrosine kinase inhibitors	Inhibit VEGFR, fibroblast growth factor receptors, platelet-derived growth factor receptors, c-Kit and Ret, resulting in inhibiting tumor angiogenesis and growth	[211]
α -solanine	EMT and MMPs	Blocking EMT and MMPs expression	[212]
Microtubule-destabilizing agents	Microtubule-cytoskeleton-mechanical forces	Inhibit microtubule polymerization at high concentrations, modulation of microtubule dynamics influence cytoskeleton	[213]
Microtubule-stabilizing agents	Microtubule	Promote microtubule polymerization	[213]

Mycalolide B	Actin-cytoskeleton	Inhibiting G-actin polymerization and severing F-actin by binding to barbed end of actin leads to a rapid collapse of the actin cytoskeleton, impairing cancer cell motility and invasion by blocking invadopodia-mediated ECM degradation	[214]
Collagenase	Collagen protein-stiffness of ECM	Decrease collagen proteins, reduce the stiffness of ECM, increase IgG diffusion to tumor sites in penetration-resistant tumors	[68]
GsMTx4	Piezo1	Inhibit the Ca ²⁺ concentration, and alter EMT-correlated markers expression in response to mechanical stretch, influence the morphology and migration	[215]
shPTK2/PND1186	FAK	Represses YAP activation by inhibiting p-YAP ^{Y357} , leading to decreased YAP nuclear localization and activation, suppresses tumor initiation and progression	[216]
AZA1	Cdc42/RAC1 GTPase	Blocking Rac1/Cdc42-dependent cell cycle progression, cancer cell migration, and increase of cancer cell apoptosis involving down-regulation of the AKT and PAK signaling pathway	[184]
Pirfenidone	Antifibrotic	Restore biomechanical abnormalities of the tumor microenvironment, related to increased stiffness and hypo-perfusion	[217]

Tranilast	Antifibrotic	Reduce stiffness and mechanical forces, improve tumor perfusion and significantly enhance the efficacy of chemotherapy and nanomedicine by affecting CAFs.	[218]
Ketotifen	Antifibrotic	Suppressed CAFs proliferation and stiffness of the extracellular matrix accompanied by an increase in vessel perfusion in fibrosarcoma and osteosarcoma	[219]
Losartan	Angiotensin inhibition	Reduces solid stress in tumours, resulting in increased vascular perfusion. And improves drug and oxygen delivery to tumours, thereby potentiating chemotherapy and reducing hypoxia in breast and pancreatic cancer models.	[35]

1222

1223

Table 2. The classification and mechanisms of mechanobiology perturbing tumor nanotherapeutics.

Classification	Therapeutic mechanisms	Functional nanoplatform	Cargoes	Cancer type	Ref.
Interfering tumor microenvironment	Improve tumor blood vessel perfusion functionality	PEGylated liposomal	Tranilast and Doxil	Breast cancer	[220]
	Decrease collagen deposition, alleviated solid stress	Hydroxyethyl starch– Ce6 conjugate self-assembled nanoparticles	Ce6 and LY2157299	Breast cancer	[207]

	Decrease the volume of the tumor interstitial fluid to ameliorate the transfer resistance derived from the high tumor interstitial fluid pressure	Graphitic carbon nitride nanosheets	DOX and luminol	Cervical carcinoma	[208]
	Reduce mechanical stresses to decompress tumor vessels and improve perfusion and chemotherapy	Pegylated liposomal	DOX	Breast cancer	[221]
Interfering cell membrane	Decrease membrane tension and increase endocytosis and tumor penetration.	Lipid nanoparticles	siRNA, mRNA, and targeted sgRNA	Ovarian cancer, and lung adenocarcinoma	[205]
	Acid-activatable disrupt cellular membrane integrity	Host defense peptides polymeric mimetic micelle	/	Pancreatic cancer	[206]
Interfering cytoskeletal	Reduce cell stiffness and inhibit cell migration through the graphene oxide nanosheets-mediated disruption of the intracellular cytoskeleton	Graphene oxide nanosheets /		Breast cancer	[222]
	Softening cells enhances nanoparticle uptake through activating clathrin- and caveolae-	Nitrogen-doped graphene quantum dots	DOX	Breast cancer	[223]

mediated endocytosis					
Interfering glyocalyx	Dynamic stretch forces combined with stiffness changes in the interstitium alter glyocalyx gene expression, thus change the cell uptake efficiency	Liposomal nanoparticles	Dil or DiO	Lung adenocarcinoma	[224]
Interfering primary ciliary	Inhibit primary cilia related signal lysophosphatidic acid signaling Control the movement and function of a cilium with an external magnetic field, and improved cardiac function	PEG-PLGA nanoparticles CT-Fe ₂ O ₃ -NPs	Ki16425 Fenoldopam	Glioblastoma LLC-PK1	[195] [196]
Interfering mechanotransduction proteins	Inactivate Yes-associated protein and regulate Hippo signaling pathway	Ruthenium-complex-peptide / precursor molecule		Ovarian cancer	[193]

1224

1225

Table 3. Clinical trials based on mechanical forces for tumor treatment.

Drugs	Cancer type	Indication	Tips	Ref
IAG933	Mesothelioma	NF2/LATS1/LATS2 mutated tumors and tumors with functional YAP/TAZ fusions	NCT04857372, Phase I, Recruiting	[62]

VT3989	Mesothelioma	Metastatic solid tumors that are resistant or refractory to standard therapy or for which no effective standard therapy	NCT04665206, Phase I, Recruiting	[62]
ION537	Advanced solid tumors	Molecularly selected advanced solid tumors	NCT04659096, Phase I, Completed	[225]
IK-930	Solid tumors	Malignant pleural mesothelioma, epithelioid hemangioendothelioma, NF2 deficient solid tumors, and solid tumors with YAP1/TAZ fusion genes	NCT05228015, Phase I, Terminated	[226]
VS-6063	Pancreatic Ductal adenocarcinoma	Resectable pancreatic ductal adenocarcinoma	NCT03727880, Phase II, Recruiting	[227]
VS-6766	Non-small cell lung cancer	Recurrent KRAS-mutant and BRAF-mutant non-small cell lung cancer	NCT04620330, Phase II, Completed	[228]
ADH-1	Melanoma	Advanced in-transit malignant melanoma	NCT00421811, Phase II, Completed	[229]
ADH-1	Solid tumors	Incurable solid tumors expressing N-cadherin	NCT00265057, Phase II, Completed	[229]
TG-0054	Hematological tumors	Multiple myeloma, and non-hodgkin lymphoma	NCT01458288, Phase II, Completed	[230]
PF-03732010	Solid tumors	Advanced solid tumors	NCT00557505, Phase I, Completed	[231]
CHM-2101	Advanced gastrointestinal cancer	Advanced gastrointestinal cancers resistant to at least one standard treatment in the metastatic or locally advanced setting.	NCT06055439, Phase I/II, Recruiting	[232]

Maraviroc	Colorectal cancer	Advanced colorectal cancer patients with hepatic liver metastases	NCT01736813	[169]
MBQ-167	Breast cancer	Breast cancer stage IV	NCT06075810, Phase I, Recruiting	[233]
SST0001	Multiple myeloma	Advanced refractory multiple myeloma	NCT01764880, Phase I, Completed	[234]

1226

1227

1228

1229

1230

1231

1232
1233
1234
1235
1236
1237
1238
1239
1240
1241
1242
1243
1244
1245
1246
1247
1248
1249
1250
1251
1252
1253
1254
1255
1256
1257
1258
1259
1260
1261
1262
1263
1264
1265
1266
1267
1268
1269
1270
1271
1272
1273
1274
1275

Reference:

1. Pfister SX, Ashworth A. Marked for death: targeting epigenetic changes in cancer. *Nat Rev Drug Discov.* 2017; 16: 241-63.
2. Liu Q, Luo Q, Ju Y, Song G. Role of the mechanical microenvironment in cancer development and progression. *Cancer Biol Med.* 2020; 17: 282-92.
3. Händel C, Schmidt BUS, Schiller J, Dietrich U, Möhn T, Kießling TR, et al. Cell membrane softening in human breast and cervical cancer cells. *New J Phys.* 2015; 17: 083008.
4. Braig S, Sebastian Schmidt BU, Stoiber K, Händel C, Möhn T, Werz O, et al. Pharmacological targeting of membrane rigidity: implications on cancer cell migration and invasion. *New J Phys.* 2015; 17: 083007.
5. Massey A, Stewart J, Smith C, Parvini C, McCormick M, Do K, et al. Mechanical properties of human tumour tissues and their implications for cancer development. *Nat Rev Phys.* 2024; 6: 269-82.
6. Suresh S. Biomechanics and biophysics of cancer cells. *Acta Biomater.* 2007; 3: 413-38.
7. Wu PH, Aroush DR, Asnacios A, Chen WC, Dokukin ME, Doss BL, et al. A comparison of methods to assess cell mechanical properties. *Nat Methods.* 2018; 15: 491-8.
8. Gonzalez-Bermudez B, Guinea GV, Plaza GR. Advances in micropipette aspiration: applications in cell biomechanics, models, and extended studies. *Biophys J.* 2019; 116: 587-94.
9. Oh MJ, Kuhr F, Byfield F, Levitan I. Micropipette aspiration of substrate-attached cells to estimate cell stiffness. *J Vis Exp.* 2012; 67: 3886.
10. Bustamante CJ, Chemla YR, Liu S, Wang MD. Optical tweezers in single-molecule biophysics. *Nat Rev Methods Primers.* 2021; 1: 25.
11. Youk JH, Gweon HM, Son EJ. Shear-wave elastography in breast ultrasonography: the state of the art. *Ultrasonography.* 2017; 36: 300-9.
12. Mariappan YK, Glaser KJ, Ehman RL. Magnetic resonance elastography: a review. *Clin Anat.* 2010; 23: 497-511.
13. Wang J, Lu D, Mao D, Long M. Mechanomics: an emerging field between biology and biomechanics. *Protein Cell.* 2014; 5: 518-31.
14. Kim YS, Majid M, Melchiorri AJ, Mikos AG. Applications of decellularized extracellular matrix in bone and cartilage tissue engineering. *Bioeng Transl Med.* 2019; 4: 83-95.
15. Bao L, Kong H, Ja Y, Wang C, Qin L, Sun H, et al. The relationship between cancer and biomechanics. *Front Oncol.* 2023; 13: 1273154.
16. Stylianopoulos T, Martin JD, Chauhan VP, Jain SR, Diop-Frimpong B, Bardeesy N, et al. Causes, consequences, and remedies for growth-induced solid stress in murine and human tumors. *Proc Natl Acad Sci U S A.* 2012; 109: 15101-8.
17. Irvine KD, Shraiman BI. Mechanical control of growth: ideas, facts and challenges. *Development.* 2017; 144: 4238-48.
18. Levayer R. Solid stress, competition for space and cancer: The opposing roles of mechanical cell competition in tumour initiation and growth. *Semin Cancer Biol.* 2020; 63: 69-80.
19. Tan M, Song B, Zhao X, Du J. The role and mechanism of compressive stress in tumor. *Front Oncol.* 2024; 14: 1459313.
20. Kim BG, Gao MQ, Kang S, Choi YP, Lee JH, Kim JE, et al. Mechanical compression

1276 induces VEGFA overexpression in breast cancer via DNMT3A-dependent miR-9
1277 downregulation. *Cell Death Dis.* 2017; 8: e2646.

1278 21. Jain RK, Martin JD, Stylianopoulos T. The role of mechanical forces in tumor growth and
1279 therapy. *Annu Rev Biomed Eng.* 2014; 16: 321-46.

1280 22. Polacheck WJ, German AE, Mammoto A, Ingber DE, Kamm RD. Mechanotransduction of
1281 fluid stresses governs 3D cell migration. *Proc Natl Acad Sci U S A.* 2014; 111: 2447-52.

1282 23. Shields JD, Fleury ME, Yong C, Tomei AA, Randolph GJ, Swartz MA. Autologous
1283 chemotaxis as a mechanism of tumor cell homing to lymphatics via interstitial flow and autocrine
1284 CCR7 signaling. *Cancer Cell.* 2007; 11: 526-38.

1285 24. Hyler AR, Baudoin NC, Brown MS, Stremmer MA, Cimini D, Davalos RV, et al. Fluid shear
1286 stress impacts ovarian cancer cell viability, subcellular organization, and promotes genomic
1287 instability. *PLoS One.* 2018; 13: e0194170.

1288 25. Bates ME, Libring S, Reinhart-King CA. Forces exerted and transduced by cancer-
1289 associated fibroblasts during cancer progression. *Biol Cell.* 2023; 115: e2200104.

1290 26. Pang MF, Siedlik MJ, Han S, Stallings-Mann M, Radisky DC, Nelson CM. Tissue stiffness
1291 and hypoxia modulate the integrin-linked kinase ILK to control breast cancer stem-like cells.
1292 *Cancer Res.* 2016; 76: 5277-87.

1293 27. Ghosh K, Thodeti CK, Dudley AC, Mammoto A, Klagsbrun M, Ingber DE. Tumor-derived
1294 endothelial cells exhibit aberrant Rho-mediated mechanosensing and abnormal angiogenesis
1295 in vitro. *Proc Natl Acad Sci U S A.* 2008; 105: 11305-10.

1296 28. Bordeleau F, Mason BN, Lollis EM, Mazzola M, Zanotelli MR, Somasegar S, et al. Matrix
1297 stiffening promotes a tumor vasculature phenotype. *Proc Natl Acad Sci U S A.* 2017; 114: 492-
1298 7.

1299 29. Wendong Y, Jiali J, Qiaomei F, Yayun W, Xianze X, Zheng S, et al. Biomechanical forces
1300 and force-triggered drug delivery in tumor neovascularization. *Biomed Pharmacother.* 2024;
1301 171: 116117.

1302 30. Dong Y, Xie X, Wang Z, Hu C, Zheng Q, Wang Y, et al. Increasing matrix stiffness
1303 upregulates vascular endothelial growth factor expression in hepatocellular carcinoma cells
1304 mediated by integrin $\beta 1$. *Biochem Biophys Res Commun.* 2014; 444: 427-32.

1305 31. Wang Y, Zhang X, Wang W, Xing X, Wu S, Dong Y, et al. Integrin $\alpha v\beta 5$ /Akt/Sp1 pathway
1306 participates in matrix stiffness-mediated effects on VEGFR2 upregulation in vascular
1307 endothelial cells. *Am J Cancer Res.* 2020; 10: 2635-48.

1308 32. Amadio M, Govoni S, Pascale A. Targeting VEGF in eye neovascularization: What's new?:
1309 A comprehensive review on current therapies and oligonucleotide-based interventions under
1310 development. *Pharmacol Res.* 2016; 103: 253-69.

1311 33. Nia HT, Munn LL, Jain RK. Physical traits of cancer. *Science.* 2020; 370: eaaz0868.

1312 34. Samuel T, Rapic S, O'Brien C, Edson M, Zhong Y, DaCosta RS. Quantitative intravital
1313 imaging for real-time monitoring of pancreatic tumor cell hypoxia and stroma in an orthotopic
1314 mouse model. *Sci Adv.* 2023; 9: eade8672.

1315 35. Chauhan VP, Martin JD, Liu H, Lacorre DA, Jain SR, Kozin SV, et al. Angiotensin inhibition
1316 enhances drug delivery and potentiates chemotherapy by decompressing tumour blood vessels.
1317 *Nat Commun.* 2013; 4: 2516.

1318 36. Boucher Y, Leunig M, Jain RK. Tumor angiogenesis and interstitial hypertension. *Cancer*
1319 *Res.* 1996; 56: 4264-6.

- 1320 37. Padera TP, Stoll BR, Tooredman JB, Capen D, di Tomaso E, Jain RK. Pathology: cancer
1321 cells compress intratumour vessels. *Nature*. 2004; 427: 695.
- 1322 38. Grivennikov SI, Greten FR, Karin M. Immunity, inflammation, and cancer. *Cell*. 2010; 140:
1323 883-99.
- 1324 39. Lietz M, Dreesmann L, Hoss M, Oberhoffner S, Schlosshauer B. Neuro tissue engineering
1325 of glial nerve guides and the impact of different cell types. *Biomaterials*. 2006; 27: 1425-36.
- 1326 40. Jain RK. Normalizing tumor microenvironment to treat cancer: bench to bedside to
1327 biomarkers. *J Clin Oncol*. 2013; 31: 2205-18.
- 1328 41. Sun C, Jain RK, Munn LL. Non-uniform plasma leakage affects local hematocrit and blood
1329 flow: implications for inflammation and tumor perfusion. *Ann Biomed Eng*. 2007; 35: 2121-9.
- 1330 42. Pries AR, Höpfner M, le Noble F, Dewhirst MW, Secomb TW. The shunt problem: control
1331 of functional shunting in normal and tumour vasculature. *Nat Rev Cancer*. 2010; 10: 587-93.
- 1332 43. Kamoun WS, Chae SS, Lacorre DA, Tyrrell JA, Mitre M, Gillissen MA, et al. Simultaneous
1333 measurement of RBC velocity, flux, hematocrit and shear rate in vascular networks. *Nat*
1334 *Methods*. 2010; 7: 655-60.
- 1335 44. Yuan F, Salehi HA, Boucher Y, Vasthare US, Tuma RF, Jain RK. Vascular permeability and
1336 microcirculation of gliomas and mammary carcinomas transplanted in rat and mouse cranial
1337 windows. *Cancer Res*. 1994; 54: 4564-8.
- 1338 45. Galie PA, Nguyen DH, Choi CK, Cohen DM, Janmey PA, Chen CS. Fluid shear stress
1339 threshold regulates angiogenic sprouting. *Proc Natl Acad Sci U S A*. 2014; 111: 7968-73.
- 1340 46. Coon BG, Baeyens N, Han J, Budatha M, Ross TD, Fang JS, et al. Intramembrane binding
1341 of VE-cadherin to VEGFR2 and VEGFR3 assembles the endothelial mechanosensory complex.
1342 *J Cell Biol*. 2015; 208: 975-86.
- 1343 47. Zanotelli MR, Reinhart-King CA. Mechanical forces in tumor angiogenesis. In: Dong C,
1344 Zahir N, Konstantopoulos K, Eds. *BIOMECHANICS IN ONCOLOGY*, 1st ed. Cham: Springer;
1345 2018:91-112.
- 1346 48. Yang S, Fei W, Zhao Y, Wang F, Ye Y, Wang F. Combat against gynecological cancers with
1347 blood vessels as entry point: anti-angiogenic drugs, clinical trials and pre-clinical nano-delivery
1348 platforms. *Int J Nanomedicine*. 2023; 18: 3035-46.
- 1349 49. Gensbittel V, Krater M, Harlepp S, Busnelli I, Guck J, Goetz JG. Mechanical adaptability
1350 of tumor cells in metastasis. *Dev Cell*. 2021; 56: 164-79.
- 1351 50. Gargalionis AN, Papavassiliou KA, Papavassiliou AG. Mechanobiology of solid tumors.
1352 *Biochim Biophys Acta Mol Basis Dis*. 2022; 1868: 166555.
- 1353 51. Zhovmer AS, Manning A, Smith C, Hayes JB, Burnette DT, Wang J, et al. Mechanical
1354 counterbalance of kinesin and dynein motors in a microtubular network regulates cell
1355 mechanics, 3D architecture, and mechanosensing. *ACS Nano*. 2021; 15: 17528-48.
- 1356 52. Swaminathan V, Mythreye K, O'Brien ET, Berchuck A, Globe GC, Superfine R. Mechanical
1357 stiffness grades metastatic potential in patient tumor cells and in cancer cell lines. *Cancer Res*.
1358 2011; 71: 5075-80.
- 1359 53. Ferrara B, Pignatelli C, Cossutta M, Citro A, Courty J, Piemonti L. The extracellular matrix
1360 in pancreatic cancer: description of a complex network and promising therapeutic options.
1361 *Cancers (Basel)*. 2021; 13: 4442.
- 1362 54. Yang Z, Zhou L, Si T, Chen S, Liu C, Ng KK, et al. Lysyl hydroxylase LH1 promotes
1363 confined migration and metastasis of cancer cells by stabilizing Septin2 to enhance actin

1364 network. *Mol Cancer*. 2023; 22: 21.

1365 55. Mistriotis P, Wisniewski EO, Bera K, Keys J, Li Y, Tuntithavornwat S, et al. Confinement
1366 hinders motility by inducing RhoA-mediated nuclear influx, volume expansion, and blebbing. *J*
1367 *Cell Biol*. 2019; 218: 4093-111.

1368 56. Keys J, Cheung BCH, Elpers MA, Wu M, Lammerding J. Rear cortex contraction aids in
1369 nuclear transit during confined migration by increasing pressure in the cell posterior. *J Cell Sci*.
1370 2024; 137: jcs260623.

1371 57. Ahn EH, Kim Y, Kshitiz, An SS, Afzal J, Lee S, et al. Spatial control of adult stem cell fate
1372 using nanotopographic cues. *Biomaterials*. 2014; 35: 2401-10.

1373 58. Haschka MD, Karbon G, Soratroi C, O'Neill KL, Luo X, Villunger A. MARCH5-dependent
1374 degradation of MCL1/NOXA complexes defines susceptibility to antimitotic drug treatment. *Cell*
1375 *Death Differ*. 2020; 27: 2297-312.

1376 59. Diouf B, Crews KR, Lew G, Pei D, Cheng C, Bao J, et al. Association of an inherited genetic
1377 variant with vincristine-related peripheral neuropathy in children with acute lymphoblastic
1378 leukemia. *Jama*. 2015; 313: 815-23.

1379 60. van Tienderen GS, Rosmark O, Lieshout R, Willemse J, de Weijer F, Elowsson Rendin L,
1380 et al. Extracellular matrix drives tumor organoids toward desmoplastic matrix deposition and
1381 mesenchymal transition. *Acta Biomater*. 2023; 158: 115-31.

1382 61. Sleeboom JJF, van Tienderen GS, Schenke-Layland K, van der Laan LJW, Khalil AA,
1383 Verstegen MMA. The extracellular matrix as hallmark of cancer and metastasis: From
1384 biomechanics to therapeutic targets. *Sci Transl Med*. 2024; 16: eadg3840.

1385 62. Kalli M, Poskus MD, Stylianopoulos T, Zervantonakis IK. Beyond matrix stiffness: targeting
1386 force-induced cancer drug resistance. *Trends Cancer*. 2023; 9: 937-54.

1387 63. Wu J, Chen J, Feng Y, Tian H, Chen X. Tumor microenvironment as the "regulator" and
1388 "target" for gene therapy. *J Gene Med*. 2019; 21: e3088.

1389 64. Barbazan J, Matic Vignjevic D. Cancer associated fibroblasts: is the force the path to the
1390 dark side? *Curr Opin Cell Biol*. 2019; 56: 71-9.

1391 65. Liu QP, Luo Q, Deng B, Ju Y, Song GB. Stiffer matrix accelerates migration of
1392 hepatocellular carcinoma cells through enhanced aerobic glycolysis via the MAPK-YAP
1393 signaling. *Cancers (Basel)*. 2020; 12: 490.

1394 66. Huang M, Wang H, Mackey C, Chung MC, Guan J, Zheng G, et al. YAP at the crossroads
1395 of biomechanics and drug resistance in human cancer. *Int J Mol Sci*. 2023; 24: 12491.

1396 67. Medina SH, Bush B, Cam M, Sevcik E, DelRio FW, Nandy K, et al. Identification of a
1397 mechanogenetic link between substrate stiffness and chemotherapeutic response in breast
1398 cancer. *Biomaterials*. 2019; 202: 1-11.

1399 68. Netti PA, Berk DA, Swartz MA, Grodzinsky AJ, Jain RK. Role of extracellular matrix
1400 assembly in interstitial transport in solid tumors. *Cancer Res*. 2000; 60: 2497-503.

1401 69. Piccolo S, Panciera T, Contessotto P, Cordenonsi M. YAP/TAZ as master regulators in
1402 cancer: modulation, function and therapeutic approaches. *Nat Cancer*. 2023; 4: 9-26.

1403 70. Najafi M, Farhood B, Mortezaee K. Extracellular matrix (ECM) stiffness and degradation
1404 as cancer drivers. *J Cell Biochem*. 2019; 120: 2782-90.

1405 71. Lee HO, Mullins SR, Franco-Barraza J, Valianou M, Cukierman E, Cheng JD. FAP-
1406 overexpressing fibroblasts produce an extracellular matrix that enhances invasive velocity and
1407 directionality of pancreatic cancer cells. *BMC Cancer*. 2011; 11: 245.

- 1408 72. Kopecka J, Trouillas P, Gasparovic AC, Gazzano E, Assaraf YG, Riganti C. Phospholipids
1409 and cholesterol: inducers of cancer multidrug resistance and therapeutic targets. *Drug Resist*
1410 *Updat.* 2020; 49: 100670.
- 1411 73. Criscuolo D, Avolio R, Calice G, Laezza C, Paladino S, Navarra G, et al. Cholesterol
1412 homeostasis modulates platinum sensitivity in human ovarian cancer. *Cells.* 2020; 9: 828.
- 1413 74. Goebel A, Zinna VM, Dell'Endice S, Jaschke N, Kuhlmann JD, Wimberger P, et al. Anti-
1414 tumor effects of mevalonate pathway inhibition in ovarian cancer. *BMC Cancer.* 2020; 20: 703.
- 1415 75. Hendrich AB, Michalak K. Lipids as a target for drugs modulating multidrug resistance of
1416 cancer cells. *Curr Drug Targets.* 2003; 4: 23-30.
- 1417 76. Preetha A, Banerjee R, Huilgol N. Tensiometric profiles and their modulation by cholesterol:
1418 implications in cervical cancer. *Cancer invest.* 2007; 25: 172-81.
- 1419 77. Ye DM, Ye SC, Yu SQ, Shu FF, Xu SS, Chen QQ, et al. Drug-resistance reversal in
1420 colorectal cancer cells by destruction of flotillins, the key lipid rafts proteins. *Neoplasma.* 2019;
1421 66: 576-83.
- 1422 78. Zalba S, Ten Hagen TL. Cell membrane modulation as adjuvant in cancer therapy. *Cancer*
1423 *Treat Rev.* 2017; 52: 48-57.
- 1424 79. Chantemargue B, Di Meo F, Berka K, Picard N, Arnion H, Essig M, et al. Structural patterns
1425 of the human ABCC4/MRP4 exporter in lipid bilayers rationalize clinically observed
1426 polymorphisms. *Pharmacol Res.* 2018; 133: 318-27.
- 1427 80. Meyer dos Santos S, Weber CC, Franke C, Müller WE, Eckert GP. Cholesterol: Coupling
1428 between membrane microenvironment and ABC transporter activity. *Biochem Biophys Res*
1429 *Commun.* 2007; 354: 216-21.
- 1430 81. Raghavan V, Vijayaraghavalu S, Peetla C, Yamada M, Morisada M, Labhasetwar V.
1431 Sustained epigenetic drug delivery depletes cholesterol-sphingomyelin rafts from resistant
1432 breast cancer cells, influencing biophysical characteristics of membrane lipids. *Langmuir.* 2015;
1433 31: 11564-73.
- 1434 82. Tarbell JM, Cancel LM. The glycocalyx and its significance in human medicine. *J Intern*
1435 *Med.* 2016; 280: 97-113.
- 1436 83. Sun Z, Guo SS, Fässler R. Integrin-mediated mechanotransduction. *J Cell Biol.* 2016; 215:
1437 445-56.
- 1438 84. Paszek MJ, Boettiger D, Weaver VM, Hammer DA. Integrin clustering is driven by
1439 mechanical resistance from the glycocalyx and the substrate. *PLoS Comput Biol.* 2009; 5:
1440 e1000604.
- 1441 85. Paszek MJ, DuFort CC, Rossier O, Bainer R, Mouw JK, Godula K, et al. The cancer
1442 glycocalyx mechanically primes integrin-mediated growth and survival. *Nature.* 2014; 511: 319-
1443 25.
- 1444 86. Massey AE, Doxtater KA, Yallapu MM, Chauhan SC. Biophysical changes caused by
1445 altered MUC13 expression in pancreatic cancer cells. *Micron.* 2020; 130: 102822.
- 1446 87. Qazi H, Palomino R, Shi ZD, Munn LL, Tarbell JM. Cancer cell glycocalyx mediates
1447 mechanotransduction and flow-regulated invasion. *Integr Biol (Camb).* 2013; 5: 1334-43.
- 1448 88. Yates TJ, Lopez LE, Lokeshwar SD, Ortiz N, Kallifatidis G, Jordan A, et al. Dietary
1449 supplement 4-methylumbelliferone: an effective chemopreventive and therapeutic agent for
1450 prostate cancer. *J Natl Cancer Inst.* 2015; 107: djv085.
- 1451 89. Finlayson M. Modulation of CD44 Activity by A6-Peptide. *Front Immunol.* 2015; 6: 135.

- 1452 90. Zhao H, Wu L, Yan G, Chen Y, Zhou M, Wu Y, et al. Inflammation and tumor progression:
1453 signaling pathways and targeted intervention. *Signal Transduct Target Ther.* 2021; 6: 2426-71.
- 1454 91. Olivo Pimentel V, Yaromina A, Marcus D, Dubois LJ, Lambin P. A novel co-culture assay
1455 to assess anti-tumor CD8(+) T cell cytotoxicity via luminescence and multicolor flow cytometry.
1456 *J Immunol Methods.* 2020; 487: 112899.
- 1457 92. [No authors listed]. *Advancing cancer therapy.* *Nat Cancer.* 2021; 2: 245-6.
- 1458 93. Mill P, Christensen ST, Pedersen LB. Primary cilia as dynamic and diverse signalling hubs
1459 in development and disease. *Nat Rev Genet.* 2023; 24: 421-41.
- 1460 94. Khayyeri H, Barreto S, Lacroix D. Primary cilia mechanics affects cell mechanosensation:
1461 A computational study. *J Theor Biol.* 2015; 379: 38-46.
- 1462 95. Higgins M, Obaidi I, McMorrow T. Primary cilia and their role in cancer. *Oncol Lett.* 2019;
1463 17: 3041-7.
- 1464 96. Lee KH. Primary cilia: a novel research approach to overcome anticancer drug resistance.
1465 *Front Mol Biosci.* 2023; 10: 1270639.
- 1466 97. Peixoto E, Jin S, Thelen K, Biswas A, Richard S, Morleo M, et al. HDAC6-dependent
1467 ciliophagy is involved in ciliary loss and cholangiocarcinoma growth in human cells and murine
1468 models. *Am J Physiol Gastrointest Liver Physiol.* 2020; 318: G1022-g33.
- 1469 98. Emoto K, Masugi Y, Yamazaki K, Effendi K, Tsujikawa H, Tanabe M, et al. Presence of
1470 primary cilia in cancer cells correlates with prognosis of pancreatic ductal adenocarcinoma.
1471 *Hum Pathol.* 2014; 45: 817-25.
- 1472 99. Martínez-Hernández R, Serrano-Somavilla A, Fernández-Contreras R, Sanchez-Guerrero
1473 C, Sánchez de la Blanca N, Sacristán-Gómez P, et al. Primary cilia as a tumor marker in
1474 pituitary neuroendocrine tumors. *Mod Pathol.* 2024; 37: 100475.
- 1475 100. Kim SO, Kim BY, Lee KH. Synergistic effect of anticancer drug resistance and Wnt3a on
1476 primary ciliogenesis in A549 cell-derived anticancer drug-resistant subcell lines. *Biochem*
1477 *Biophys Res Commun.* 2022; 635: 1-11.
- 1478 101. Sanyour HJ, Li N, Rickel AP, Torres HM, Anderson RH, Miles MR, et al. Statin-mediated
1479 cholesterol depletion exerts coordinated effects on the alterations in rat vascular smooth muscle
1480 cell biomechanics and migration. *J Physiol.* 2020; 598: 1505-22.
- 1481 102. Krieg M, Dunn AR, Goodman MB. Mechanical control of the sense of touch by β -spectrin.
1482 *Nat Cell Biol.* 2014; 16: 224-33.
- 1483 103. Pollard TD, Borisy GG. Cellular motility driven by assembly and disassembly of actin
1484 filaments. *Cell.* 2003; 112: 453-65.
- 1485 104. Civelekoglu-Scholey G, Scholey JM. Mitotic force generators and chromosome
1486 segregation. *Cell Mol Life Sci.* 2010; 67: 2231-50.
- 1487 105. Tang Y, He Y, Zhang P, Wang J, Fan C, Yang L, et al. LncRNAs regulate the cytoskeleton
1488 and related Rho/ROCK signaling in cancer metastasis. *Mol Cancer.* 2018; 17: 77.
- 1489 106. Xin Y, Li K, Huang M, Liang C, Siemann D, Wu L, et al. Biophysics in tumor growth and
1490 progression: from single mechano-sensitive molecules to mechanomedicine. *Oncogene.* 2023;
1491 42: 3457-90.
- 1492 107. Chen X, Xu Z, Tang K, Hu G, Du P, Wang J, et al. The mechanics of tumor cells dictate
1493 malignancy via cytoskeleton-mediated APC/Wnt/ β -catenin signaling. *Research (Wash D C).*
1494 2023; 6: 0224.
- 1495 108. Wirtz D, Konstantopoulos K, Searson PC. The physics of cancer: the role of physical

1496 interactions and mechanical forces in metastasis. *Nat Rev Cancer*. 2011; 11: 512-22.

1497 109. Liu L, Jiang H, Zhao W, Meng Y, Li J, Huang T, et al. Cdc42-mediated supracellular
1498 cytoskeleton induced cancer cell migration under low shear stress. *Biochem Biophys Res*
1499 *Commun*. 2019; 519: 134-40.

1500 110. Tang K, Xin Y, Li K, Chen X, Tan Y. Cell cytoskeleton and stiffness are mechanical
1501 indicators of organotropism in breast cancer. *Biology-Basel*. 2021; 10: 259.

1502 111. Heo SJ, Cosgrove BD, Dai EN, Mauck RL. Mechano-adaptation of the stem cell nucleus.
1503 *Nucleus*. 2018; 9: 9-19.

1504 112. Kirby TJ, Lammerding J. Emerging views of the nucleus as a cellular mechanosensor. *Nat*
1505 *Cell Biol*. 2018; 20: 373-81.

1506 113. Shi H, Zhou K, Wang M, Wang N, Song Y, Xiong W, et al. Integrating physicommechanical
1507 and biological strategies for BTE: biomaterials-induced osteogenic differentiation of MSCs.
1508 *Theranostics*. 2023; 13: 3245-75.

1509 114. Swift J, Ivanovska IL, Buxboim A, Harada T, Dingal PC, Pinter J, et al. Nuclear lamin-A
1510 scales with tissue stiffness and enhances matrix-directed differentiation. *Science*. 2013; 341:
1511 1240104.

1512 115. Malviya AN, Rogue PJ. "Tell me where is calcium bred": clarifying the roles of nuclear
1513 calcium. *Cell*. 1998; 92: 17-23.

1514 116. Enyedi B, Jelcic M, Niethammer P. The cell nucleus serves as a mechanotransducer of
1515 tissue damage-induced inflammation. *Cell*. 2016; 165: 1160-70.

1516 117. Heo SJ, Thorpe SD, Driscoll TP, Duncan RL, Lee DA, Mauck RL. Biophysical regulation of
1517 chromatin architecture instills a mechanical memory in mesenchymal stem cells. *Sci Rep*. 2015;
1518 5: 16895.

1519 118. Heo SJ, Han WM, Szczesny SE, Cosgrove BD, Elliott DM, Lee DA, et al. Mechanically
1520 induced chromatin condensation requires cellular contractility in mesenchymal stem cells.
1521 *Biophys J*. 2016; 111: 864-74.

1522 119. Greene JM, Schneble EJ, Jackson DO, Hale DF, Vreeland TJ, Flores M, et al. A phase I/IIa
1523 clinical trial in stage IV melanoma of an autologous tumor-dendritic cell fusion (dendritoma)
1524 vaccine with low dose interleukin-2. *Cancer Immunol Immunother*. 2016; 65: 383-92.

1525 120. Jain N, Iyer KV, Kumar A, Shivashankar GV. Cell geometric constraints induce modular
1526 gene-expression patterns via redistribution of HDAC3 regulated by actomyosin contractility.
1527 *Proc Natl Acad Sci U S A*. 2013; 110: 11349-54.

1528 121. Baarlink C, Wang H, Grosse R. Nuclear actin network assembly by formins regulates the
1529 SRF coactivator MAL. *Science*. 2013; 340: 864-7.

1530 122. Denais CM, Gilbert RM, Isermann P, McGregor AL, te Lindert M, Weigel B, et al. Nuclear
1531 envelope rupture and repair during cancer cell migration. *Science*. 2016; 352: 353-8.

1532 123. Dahl KN, Scaffidi P, Islam MF, Yodh AG, Wilson KL, Misteli T. Distinct structural and
1533 mechanical properties of the nuclear lamina in Hutchinson-Gilford progeria syndrome. *Proc Natl*
1534 *Acad Sci U S A*. 2006; 103: 10271-6.

1535 124. Nava MM, Miroshnikova YA, Biggs LC, Whitefield DB, Metge F, Boucas J, et al.
1536 Heterochromatin-driven nuclear softening protects the genome against mechanical stress-
1537 induced damage. *Cell*. 2020; 181: 800-17.e22.

1538 125. dos Santos A, Toseland CP. Regulation of nuclear mechanics and the impact on DNA
1539 damage. *Int J Mol Sci*. 2021; 22: 3178.

1540 126. Panciera T, Azzolin L, Cordenonsi M, Piccolo S. Mechanobiology of YAP and TAZ in
1541 physiology and disease. *Nat Rev Mol Cell Biol.* 2017; 18: 758-70.

1542 127. Shapovalov G, Ritaine A, Skryma R, Prevarskaya N. Role of TRP ion channels in cancer
1543 and tumorigenesis. *Semin Immunopathol.* 2016; 38: 357-69.

1544 128. Chachisvilis M, Zhang YL, Frangos JA. G protein-coupled receptors sense fluid shear
1545 stress in endothelial cells. *Proc Natl Acad Sci U S A.* 2006; 103: 15463-8.

1546 129. He L, Si G, Huang J, Samuel ADT, Perrimon N. Mechanical regulation of stem-cell
1547 differentiation by the stretch-activated Piezo channel. *Nature.* 2018; 555: 103-6.

1548 130. Cooper J, Giancotti FG. Integrin Signaling in Cancer: Mechanotransduction, stemness,
1549 epithelial plasticity, and therapeutic resistance. *Cancer Cell.* 2019; 35: 347-67.

1550 131. Sulzmaier FJ, Jean C, Schlaepfer DD. FAK in cancer: mechanistic findings and clinical
1551 applications. *Nat Rev Cancer.* 2014; 14: 598-610.

1552 132. Seetharaman S, Etienne-Manneville S. Integrin diversity brings specificity in
1553 mechanotransduction. *Biol Cell.* 2018; 110: 49-64.

1554 133. Shen B, Delaney MK, Du X. Inside-out, outside-in, and inside-outside-in: G protein
1555 signaling in integrin-mediated cell adhesion, spreading, and retraction. *Curr Opin Cell Biol.* 2012;
1556 24: 600-6.

1557 134. Navab R, Strumpf D, To C, Pasko E, Kim KS, Park CJ, et al. Integrin $\alpha 11\beta 1$ regulates
1558 cancer stromal stiffness and promotes tumorigenicity and metastasis in non-small cell lung
1559 cancer. *Oncogene.* 2016; 35: 1899-908.

1560 135. Luo CW, Wu CC, Ch'ang HJ. Radiation sensitization of tumor cells induced by shear stress:
1561 the roles of integrins and FAK. *Biochim Biophys Acta.* 2014; 1843: 2129-37.

1562 136. Lu P, Weaver VM, Werb Z. The extracellular matrix: a dynamic niche in cancer progression.
1563 *J Cell Biol.* 2012; 196: 395-406.

1564 137. Zhang W, Wang J, Liu C, Li Y, Sun C, Wu J, et al. Crosstalk and plasticity driving between
1565 cancer-associated fibroblasts and tumor microenvironment: significance of breast cancer
1566 metastasis. *J Transl Med.* 2023; 21: 827.

1567 138. Levental KR, Yu H, Kass L, Lakins JN, Egeblad M, Erler JT, et al. Matrix crosslinking forces
1568 tumor progression by enhancing integrin signaling. *Cell.* 2009; 139: 891-906.

1569 139. Giancotti FG, Ruoslahti E. Elevated levels of the alpha 5 beta 1 fibronectin receptor
1570 suppress the transformed phenotype of Chinese hamster ovary cells. *Cell.* 1990; 60: 849-59.

1571 140. Iwanicki MP, Chen H-Y, Iavarone C, Zervantonakis IK, Muranen T, Novak M, et al. Mutant
1572 p53 regulates ovarian cancer transformed phenotypes through autocrine matrix deposition. *Jci*
1573 *Insight.* 2016; 1: e86829.

1574 141. Guo W, Giancotti FG. Integrin signalling during tumour progression. *Nat Rev Mol Cell Biol.*
1575 2004; 5: 816-26.

1576 142. Slack RJ, Macdonald SJF, Roper JA, Jenkins RG, Hatley RJD. Emerging therapeutic
1577 opportunities for integrin inhibitors. *Nat Rev Drug Discov.* 2022; 21: 60-78.

1578 143. Zhang Y, Du J, Liu X, Shang F, Deng Y, Ye J, et al. Multi-domain interaction mediated
1579 strength-building in human alpha-actinin dimers unveiled by direct single-molecule
1580 quantification. *Nat Commun.* 2024; 15: 6151.

1581 144. Drees F, Pokutta S, Yamada S, Nelson WJ, Weis WI. Alpha-catenin is a molecular switch
1582 that binds E-cadherin-beta-catenin and regulates actin-filament assembly. *Cell.* 2005; 123: 903-
1583 15.

1584 145. Spill F, Reynolds DS, Kamm RD, Zaman MH. Impact of the physical microenvironment on
1585 tumor progression and metastasis. *Curr Opin Biotechnol.* 2016; 40: 41-8.

1586 146. Yonemura S, Wada Y, Watanabe T, Nagafuchi A, Shibata M. alpha-Catenin as a tension
1587 transducer that induces adherens junction development. *Nat Cell Biol.* 2010; 12: 533-42.

1588 147. Shen KH, Liao AC, Hung JH, Lee WJ, Hu KC, Lin PT, et al. alpha-Solanine inhibits invasion
1589 of human prostate cancer cell by suppressing epithelial-mesenchymal transition and MMPs
1590 expression. *Molecules.* 2014; 19: 11896-914.

1591 148. Lawler K, O'Sullivan G, Long A, Kenny D. Shear stress induces internalization of E-
1592 cadherin and invasiveness in metastatic oesophageal cancer cells by a Src-dependent pathway.
1593 *Cancer Sci.* 2009; 100: 1082-7.

1594 149. Reid SE, Kay EJ, Neilson LJ, Henze AT, Serneels J, McGhee EJ, et al. Tumor matrix
1595 stiffness promotes metastatic cancer cell interaction with the endothelium. *EMBO J.* 2017; 36:
1596 2373-89.

1597 150. Benham-Pyle BW, Pruitt BL, Nelson WJ. Cell adhesion. Mechanical strain induces E-
1598 cadherin-dependent Yap1 and beta-catenin activation to drive cell cycle entry. *Science.* 2015;
1599 348: 1024-7.

1600 151. Zhang Q, Lin F, Huang JY, Xiong CY. Mechanical transmission enables EMT cancer cells
1601 to drive epithelial cancer cell migration to guide tumor spheroid disaggregation. *Sci China Life*
1602 *Sci.* 2022; 65: 2031-49.

1603 152. Petho Z, Najder K, Bulk E, Schwab A. Mechanosensitive ion channels push cancer
1604 progression. *Cell Calcium.* 2019; 80: 79-90.

1605 153. Coste B, Mathur J, Schmidt M, Earley TJ, Ranade S, Petrus MJ, et al. Piezo1 and Piezo2
1606 are essential components of distinct mechanically activated cation channels. *Science.* 2010;
1607 330: 55-60.

1608 154. Luo M, Cai G, Ho KKY, Wen K, Tong Z, Deng L, et al. Compression enhances invasive
1609 phenotype and matrix degradation of breast Cancer cells via Piezo1 activation. *BMC Mol Cell*
1610 *Biol.* 2022; 23: 1.

1611 155. Lai A, Cox CD, Chandra Sekar N, Thurgood P, Jaworowski A, Peter K, et al.
1612 Mechanosensing by Piezo1 and its implications for physiology and various pathologies. *Biol*
1613 *Rev Camb Philos Soc.* 2022; 97: 604-14.

1614 156. Chen X, Wanggou S, Bodalia A, Zhu M, Dong W, Fan JJ, et al. A feedforward mechanism
1615 mediated by mechanosensitive ion channel PIEZO1 and tissue mechanics promotes glioma
1616 aggression. *Neuron.* 2018; 100: 799-815 e7.

1617 157. Tijore A, Yao M, Wang YH, Hariharan A, Nematbakhsh Y, Lee Doss B, et al. Selective
1618 killing of transformed cells by mechanical stretch. *Biomaterials.* 2021; 275: 120866.

1619 158. Li X, Cheng Y, Wang Z, Zhou J, Jia Y, He X, et al. Calcium and TRPV4 promote metastasis
1620 by regulating cytoskeleton through the RhoA/ROCK1 pathway in endometrial cancer. *Cell*
1621 *Death Dis.* 2020; 11: 1009.

1622 159. Momin A, Bahrapour S, Min HK, Chen X, Wang X, Sun Y, et al. Channeling force in the
1623 brain: mechanosensitive ion channels choreograph mechanics and malignancies. *Trends*
1624 *Pharmacol Sci.* 2021; 42: 367-84.

1625 160. Liu L, Wu N, Wang Y, Zhang X, Xia B, Tang J, et al. TRPM7 promotes the epithelial-
1626 mesenchymal transition in ovarian cancer through the calcium-related PI3K / AKT oncogenic
1627 signaling. *J Exp Clin Cancer Res.* 2019; 38: 106.

1628 161. Krzak G, Willis CM, Smith JA, Pluchino S, Peruzzotti-Jametti L. Succinate receptor 1: an
1629 emerging regulator of myeloid cell function in inflammation. *Trends Immunol.* 2021; 42: 45-58.
1630 162. Dela Paz NG, Melchior B, Frangos JA. Shear stress induces G α (q/11) activation
1631 independently of G protein-coupled receptor activation in endothelial cells. *Am J Physiol Cell*
1632 *Physiol.* 2017; 312: C428-c37.
1633 163. Li X, Wang J. Mechanical tumor microenvironment and transduction: cytoskeleton
1634 mediates cancer cell invasion and metastasis. *Int J Biol Sci.* 2020; 16: 2014-28.
1635 164. Yang N, Chen T, Wang L, Liu R, Niu Y, Sun L, et al. CXCR4 mediates matrix stiffness-
1636 induced downregulation of UBTD1 driving hepatocellular carcinoma progression via YAP
1637 signaling pathway. *Theranostics.* 2020; 10: 5790-801.
1638 165. Dorsam RT, Gutkind JS. G-protein-coupled receptors and cancer. *Nat Rev Cancer.* 2007;
1639 7: 79-94.
1640 166. Liu Y, An S, Ward R, Yang Y, Guo XX, Li W, et al. G protein-coupled receptors as promising
1641 cancer targets. *Cancer Lett.* 2016; 376: 226-39.
1642 167. Lappano R, Maggiolini M. Pharmacotherapeutic targeting of G protein-coupled receptors
1643 in oncology: examples of approved therapies and emerging concepts. *Drugs.* 2017; 77: 951-
1644 65.
1645 168. van Deventer HW, O'Connor W, Jr., Brickey WJ, Aris RM, Ting JP, Serody JS. C-C
1646 chemokine receptor 5 on stromal cells promotes pulmonary metastasis. *Cancer Res.* 2005; 65:
1647 3374-9.
1648 169. Halama N, Zoernig I, Berthel A, Kahlert C, Klupp F, Suarez-Carmona M, et al. Tumoral
1649 immune cell exploitation in colorectal cancer metastases can be targeted effectively by anti-
1650 CCR5 therapy in cancer patients. *Cancer Cell.* 2016; 29: 587-601.
1651 170. Almeria CVP, Setiawan IM, Siderius M, Smit MJ. G protein-coupled receptors as promising
1652 targets in cancer. *Curr Opin Endocr Metab Res.* 2021; 16: 119-27.
1653 171. Hong SP, Yang MJ, Cho H, Park I, Bae H, Choe K, et al. Distinct fibroblast subsets regulate
1654 lacteal integrity through YAP/TAZ-induced VEGF-C in intestinal villi. *Nat Commun.* 2020; 11:
1655 4102.
1656 172. Qiao Y, Chen J, Lim YB, Finch-Edmondson ML, Seshachalam VP, Qin L, et al. YAP
1657 regulates actin dynamics through ARHGAP29 and promotes metastasis. *Cell Rep.* 2017; 19:
1658 1495-502.
1659 173. Zanconato F, Cordenonsi M, Piccolo S. YAP/TAZ at the roots of cancer. *Cancer Cell.* 2016;
1660 29: 783-803.
1661 174. Panciera T, Citron A, Di Biagio D, Battilana G, Gandin A, Giulitti S, et al. Reprogramming
1662 normal cells into tumour precursors requires ECM stiffness and oncogene-mediated changes
1663 of cell mechanical properties. *Nat Mater.* 2020; 19: 797-806.
1664 175. Nagelkerke A, Bussink J, Rowan AE, Span PN. The mechanical microenvironment in
1665 cancer: how physics affects tumours. *Semin Cancer Biol.* 2015; 35: 62-70.
1666 176. Martellucci S, Clementi L, Sabetta S, Mattei V, Botta L, Angelucci A. Src family kinases as
1667 therapeutic targets in advanced solid tumors: what we have learned so far. *Cancers (Basel).*
1668 2020; 12: 1448.
1669 177. Crosas-Molist E, Samain R, Kohlhammer L, Orgaz JL, George SL, Maiques O, et al. Rho
1670 GTPase signaling in cancer progression and dissemination. *Physiol Rev.* 2022; 102: 455-510.
1671 178. Sahai E, Marshall CJ. RHO-GTPases and cancer. *Nat Rev Cancer.* 2002; 2: 133-42.

1672 179. Hodge RG, Ridley AJ. Regulating Rho GTPases and their regulators. *Nat Rev Mol Cell*
1673 *Biol.* 2016; 17: 496-510.

1674 180. Khosravi-Far R, Solski PA, Clark GJ, Kinch MS, Der CJ. Activation of Rac1, RhoA, and
1675 mitogen-activated protein kinases is required for Ras transformation. *Mol Cell Biol.* 1995; 15:
1676 6443-53.

1677 181. Qiu RG, Abo A, McCormick F, Symons M. Cdc42 regulates anchorage-independent growth
1678 and is necessary for Ras transformation. *Mol Cell Biol.* 1997; 17: 3449-58.

1679 182. Dyberg C, Fransson S, Andonova T, Sveinbjörnsson B, Lännerholm-Palm J, Olsen TK, et
1680 al. Rho-associated kinase is a therapeutic target in neuroblastoma. *Proc Natl Acad Sci U S A.*
1681 2017; 114: E6603-e12.

1682 183. Prudnikova TY, Rawat SJ, Chernoff J. Molecular pathways: targeting the kinase effectors
1683 of RHO-family GTPases. *Clin Cancer Res.* 2015; 21: 24-9.

1684 184. Zins K, Lucas T, Reichl P, Abraham D, Aharinejad S. A Rac1/Cdc42 GTPase-specific small
1685 molecule inhibitor suppresses growth of primary human prostate cancer xenografts and
1686 prolongs survival in mice. *PLoS One.* 2013; 8: e74924.

1687 185. Meng F, Na I, Kurgan L, Uversky VN. Compartmentalization and functionality of nuclear
1688 disorder: intrinsic disorder and protein-protein interactions in intra-nuclear compartments. *Int J*
1689 *Mol Sci.* 2016; 17: 24.

1690 186. Amin R, Shukla A, Zhu JJ, Kim S, Wang P, Tian SZ, et al. Nuclear pore protein NUP210
1691 depletion suppresses metastasis through heterochromatin-mediated disruption of tumor cell
1692 mechanical response. *Nat Commun.* 2021; 12: 7216.

1693 187. Sun H, Dong Z, Zhang Q, Liu B, Yan S, Wang Y, et al. Companion-probe & race platform
1694 for interrogating nuclear protein and migration of living cells. *Biosens Bioelectron.* 2022; 210:
1695 114281.

1696 188. Zwerger M, Ho CY, Lammerding J. Nuclear mechanics in disease. *Annu Rev Biomed Eng.*
1697 2011; 13: 397-428.

1698 189. Zwerger M, Ho CY, Lammerding J. Nuclear mechanics in disease. *Annu Rev Biomed Eng,*
1699 *Vol 13.* 2011; 13: 397-428.

1700 190. Poh YC, Shevtsov SP, Chowdhury F, Wu DC, Na S, Dundr M, et al. Dynamic force-induced
1701 direct dissociation of protein complexes in a nuclear body in living cells. *Nat Commun.* 2012; 3:
1702 866.

1703 191. Tamiello C, Kamps MA, van den Wijngaard A, Verstraeten VL, Baaijens FP, Broers JL, et
1704 al. Soft substrates normalize nuclear morphology and prevent nuclear rupture in fibroblasts
1705 from a laminopathy patient with compound heterozygous LMNA mutations. *Nucleus.* 2013; 4:
1706 61-73.

1707 192. Kaminski A, Fedorchak GR, Lammerding J. The cellular mastermind(?)
1708 mechanotransduction and the nucleus. *Prog Mol Biol Transl Sci.* 2014; 126: 157-203.

1709 193. Li G, Hu X, Nie P, Mang D, Jiao S, Zhang S, et al. Lipid-raft-targeted molecular self-
1710 assembly inactivates YAP to treat ovarian cancer. *Nano Letters.* 2021; 21: 747-55.

1711 194. Pala R, Mohieldin AM, Shamloo K, Sherpa RT, Kathem SH, Zhou J, et al. Personalized
1712 nanotherapy by specifically targeting cell organelles to improve vascular hypertension. *Nano*
1713 *Letters.* 2019; 19: 904-14.

1714 195. Loskutov YV, Griffin CL, Marinak KM, Bobko A, Margaryan NV, Geldenhuys WJ, et al. LPA
1715 signaling is regulated through the primary cilium: a novel target in glioblastoma. *Oncogene.*

1716 2018; 37: 1457-71.

1717 196. Pala R, Mohieldin AM, Sherpa RT, Kathem SH, Shamloo K, Luan Z, et al. Ciliotherapy:
1718 remote control of primary cilia movement and function by magnetic nanoparticles. *Acs Nano*.
1719 2019; 13: 3555-72.

1720 197. Samandari M, Abrinia K, Mokhtari-Dizaji M, Tamayol A. Ultrasound induced strain
1721 cytoskeleton rearrangement: An experimental and simulation study. *J Biomech*. 2017; 60: 39-
1722 47.

1723 198. Qi G, Zhang M, Tang J, Jin Y. Molecular/nanomechanical insights into electrostimulation-
1724 inhibited energy metabolism mechanisms and cytoskeleton damage of cancer cells. *Adv Sci*
1725 (Weinh). 2023; 10: e2207165.

1726 199. Yao H, Zhang L, Yan S, He Y, Zhu H, Li Y, et al. Low-intensity pulsed
1727 ultrasound/nanomechanical force generators enhance osteogenesis of BMSCs through
1728 microfilaments and TRPM7. *J Nanobiotechnology*. 2022; 20: 378.

1729 200. Song Y, Chen J, Zhang C, Xin L, Li Q, Liu Y, et al. Mechanosensitive channel Piezo1
1730 induces cell apoptosis in pancreatic cancer by ultrasound with microbubbles. *iScience*. 2022;
1731 25: 103733.

1732 201. Singh A, Tijore A, Margadant F, Simpson C, Chitkara D, Low BC, et al. Enhanced tumor
1733 cell killing by ultrasound after microtubule depolymerization. *Bioeng Transl Med*. 2021; 6:
1734 e10233.

1735 202. Van Steenberghe V, Boesmans W, Li Z, de Coene Y, Vints K, Baatsen P, et al. Molecular
1736 understanding of label-free second harmonic imaging of microtubules. *Nat Commun*. 2019; 10:
1737 3530.

1738 203. Mohammadi H, Sahai E. Mechanisms and impact of altered tumour mechanics. *Nat Cell*
1739 *Biol*. 2018; 20: 766-74.

1740 204. Seong J, Wang N, Wang Y. Mechanotransduction at focal adhesions: from physiology to
1741 cancer development. *J Cell Mol Med*. 2013; 17: 597-604.

1742 205. Zhang D, Wang G, Yu X, Wei T, Farbiak L, Johnson LT, et al. Enhancing CRISPR/Cas
1743 gene editing through modulating cellular mechanical properties for cancer therapy. *Nat*
1744 *Nanotechnol*. 2022; 17: 777-787.

1745 206. Fan F, Jin L, Yang L. PH-sensitive nanoparticles composed solely of membrane-disruptive
1746 macromolecules for treating pancreatic cancer. *ACS Appl Mater Interfaces*. 2021; 13: 12824-
1747 35.

1748 207. Chen J, Li S, Liu X, Liu S, Xiao C, Zhang Z, et al. Transforming growth factor- β blockade
1749 modulates tumor mechanical microenvironments for enhanced antitumor efficacy of
1750 photodynamic therapy. *Nanoscale*. 2021; 13: 9989-10001.

1751 208. Cong C, Rao C, Ma Z, Yu M, He Y, He Y, et al. "Nano-lymphatic" photocatalytic water-
1752 splitting for relieving tumor interstitial fluid pressure and achieving hydrodynamic therapy. *Mater*
1753 *Horiz*. 2020; 7: 3266-74.

1754 209. Cambria E, Coughlin MF, Floryan MA, Offeddu GS, Shelton SE, Kamm RD. Linking cell
1755 mechanical memory and cancer metastasis. *Nat Rev Cancer*. 2024; 24: 216-28.

1756 210. Wong KM, Horton KJ, Coveler AL, Hingorani SR, Harris WP. Targeting the tumor stroma:
1757 the biology and clinical development of pegylated recombinant human hyaluronidase
1758 (PEGPH20). *Curr Oncol Rep*. 2017; 19: 47.

1759 211. Syed YY. Anlotinib: first global approval. *Drugs*. 2018; 78: 1057-62.

1760 212. Shen KH, Liao AC, Hung JH, Lee WJ, Hu KC, Lin PT, et al. α -Solanine inhibits invasion of
1761 human prostate cancer cell by suppressing epithelial-mesenchymal transition and MMPs
1762 expression. *Molecules*. 2014; 19: 11896-914.

1763 213. Gudimchuk NB, McIntosh JR. Regulation of microtubule dynamics, mechanics and
1764 function through the growing tip. *Nat Rev Mol Cell Biol*. 2021; 22: 777-95.

1765 214. Pipaliya BV, Trofimova DN, Grange RL, Aeluri M, Deng X, Shah K, et al. Truncated actin-
1766 targeting macrolide derivative blocks cancer cell motility and invasion of extracellular matrix. *J*
1767 *Am Chem Soc*. 2021; 143: 6847-54.

1768 215. He J, Shan S, Li Q, Fang B, Xie Y. Mechanical Stretch triggers epithelial-mesenchymal
1769 transition in keratinocytes through Piezo1 channel. *Front Physiol*. 2022; 13: 745572.

1770 216. Song X, Xu H, Wang P, Wang J, Affo S, Wang H, et al. Focal adhesion kinase (FAK)
1771 promotes cholangiocarcinoma development and progression via YAP activation. *J Hepatol*.
1772 2021; 75: 888-99.

1773 217. Mpekris F, Papaphilippou PC, Panagi M, Voutouri C, Michael C, Charalambous A, et al.
1774 Pirfenidone-loaded polymeric micelles as an effective mechanotherapeutic to potentiate
1775 immunotherapy in mouse tumor models. *Acs Nano*. 2023; 17: 24654-67.

1776 218. Panagi M, Mpekris F, Chen P, Voutouri C, Nakagawa Y, Martin JD, et al. Polymeric micelles
1777 effectively reprogram the tumor microenvironment to potentiate nano-immunotherapy in mouse
1778 breast cancer models. *Nat Commun*. 2022; 13: 7165.

1779 219. Panagi M, Mpekris F, Voutouri C, Hadjigeorgiou AG, Symeonidou C, Porfyriou E, et al.
1780 Stabilizing tumor-resident mast cells restores T-cell infiltration and sensitizes sarcomas to PD-
1781 L1 inhibition. *Clin Cancer Res*. 2024; 30: 2582-97.

1782 220. Panagi M, Voutouri C, Mpekris F, Papageorgis P, Martin MR, Martin JD, et al. TGF- β
1783 inhibition combined with cytotoxic nanomedicine normalizes triple negative breast cancer
1784 microenvironment towards anti-tumor immunity. *Theranostics*. 2020; 10: 1910-22.

1785 221. Papageorgis P, Polydorou C, Mpekris F, Voutouri C, Agathokleous E, Kapnissi-
1786 Christodoulou CP, et al. Tranilast-induced stress alleviation in solid tumors improves the
1787 efficacy of chemo- and nanotherapeutics in a size-independent manner. *Sci Rep*. 2017; 7:
1788 e10233.

1789 222. Ghorbani M, Soleymani H, Hashemzadeh H, Mortezaadeh S, Sedghi M, Shojaeilangari
1790 S, et al. Microfluidic investigation of the effect of graphene oxide on mechanical properties of
1791 cell and actin cytoskeleton networks: experimental and theoretical approaches. *Sci Rep*. 2021;
1792 11: 16216.

1793 223. Chen X, Fan Y, Sun J, Zhang Z, Xin Y, Li K, et al. Nanoparticle-mediated specific
1794 elimination of soft cancer stem cells by targeting low cell stiffness. *Acta Biomater*. 2021; 135:
1795 493-505.

1796 224. Kohon AI, Man K, Mathis K, Webb J, Yang Y, Meckes B. Nanoparticle targeting of
1797 mechanically modulated glycocalyx. *bioRxiv*. 2023; 27: 2023.02.27.529887.

1798 225. Macleod AR. Abstract ND11: The discovery and characterization of ION-537: A next
1799 generation antisense oligonucleotide inhibitor of YAP1 in preclinical cancer models. *Cancer*
1800 *Res*. 2021; 81: ND11-ND.

1801 226. Tolcher AW, Lakhani NJ, McKean M, Lingaraj T, Victor L, Sanchez-Martin M, et al. A phase
1802 1, first-in-human study of IK-930, an oral TEAD inhibitor targeting the Hippo pathway in subjects
1803 with advanced solid tumors. *J Clin Oncol*. 2022; 40: TPS3168-TPS.

1804 227. Abbas AA, Davelaar J, Gai J, Brown Z, Levi A, Linden S, et al. Preliminary translational
1805 immune and stromal correlates in a randomized phase II trial of pembrolizumab with or without
1806 defactinib for resectable pancreatic ductal adenocarcinoma (PDAC). *J Clin Oncol.* 2023; 41:
1807 4024-.

1808 228. Capelletto E, Bironzo P, Denis L, Koustenis A, Bungaro M, Novello S. Single agent VS-
1809 6766 or VS-6766 plus defactinib in KRAS-mutant non-small-cell lung cancer: the RAMP-202
1810 phase II trial. *Future Oncol.* 2022; 18: 1907-15.

1811 229. Neuendorf HM, Simmons JL, Boyle GM. Therapeutic targeting of anoikis resistance in
1812 cutaneous melanoma metastasis. *Front Cell Dev Biol.* 2023; 11: 1183328.

1813 230. Yang J, Tian E, Chen L, Liu Z, Ren Y, Mao W, et al. Development and therapeutic
1814 perspectives of CXCR4 antagonists for disease therapy. *Eur J Med Chem.* 2024; 275: 116594.

1815 231. Mescher M, Jeong P, Knapp SK, Rübsam M, Saynisch M, Kranen M, et al. The epidermal
1816 polarity protein Par3 is a non-cell autonomous suppressor of malignant melanoma. *J Exp Med.*
1817 2017; 214: 339-58.

1818 232. Delaney S, Keinänen O, Lam D, Wolfe AL, Hamakubo T, Zeglis BM. Cadherin-17 as a
1819 target for the immunoPET of adenocarcinoma. *Eur J Nucl Med Mol Imaging.* 2024; 51: 2547-57.

1820 233. Medina JI, Cruz-Collazo A, Maldonado MD, Gascot TM, Borrero-Garcia LD, Cooke M, et
1821 al. Characterization of novel derivatives of MBQ-167, an inhibitor of the GTP-binding proteins
1822 Rac/Cdc42. *Cancer Res Commun.* 2022; 2: 1711-26.

1823 234. Cassinelli G, Lanzi C, Tortoreto M, Cominetti D, Petrangolini G, Favini E, et al. Antitumor
1824 efficacy of the heparanase inhibitor SST0001 alone and in combination with antiangiogenic
1825 agents in the treatment of human pediatric sarcoma models. *Biochem Pharmacol.* 2013; 85:
1826 1424-32.

1827